

interface. This latter structural event may lead to a tightening down of the FtsZ polymer spiral, much like the compression of a spring, resulting in Z-ring contraction.

Remodeling of cytoskeletal polymers is induced by transitions between nucleotide hydrolysis intermediates. The energy from hydrolysis can be used to destabilize a previously stable structure and to produce mechanical work [15, 19, 23, 43]. In organisms without a cell wall, FtsZ is the only conserved protein of the cell division machinery, suggesting that FtsZ might use GTP hydrolysis to direct cytokinesis [20, 23, 44]. Three mechanisms have been proposed for how FtsZ may transmit energy from nucleotide hydrolysis into mechanical force for constriction of the Z ring [15, 19, 23, 43]. The release of FtsZ subunits from the Z ring through depolymerization will cause the Z ring to become smaller [22], or, alternatively, FtsZ filaments may move relative to each other to reduce the circumference of the ring without depolymerization occurring, as observed for the actomyosin ring in eukaryotes [44]. In addition, the FtsZ filaments may bend upon GTP hydrolysis [43].

Since the rate-limiting step in the turnover of FtsZ polymers is GTP hydrolysis, and protofilaments consist mostly of FtsZ-GTP, GTP hydrolysis will release energy in small quanta, and will not generate a large force [23]. This situation is different from that observed for microtubules, in which almost every subunit is bound with GDP and the energy from hydrolysis is stored as strain in the polymer [33]. Perhaps microtubules need to generate a larger force because they operate on a greater geometric scale than does the Z ring [23].

Structural and Functional Homology Between FtsZ and Tubulin

The possibility that FtsZ might be a homologue of tubulin was first suggested by a short segment of its amino acid sequence, GGGTGTG, which is virtually identical to the tubulin signature motif, (G/A)GGTGSG, found in all α , β and γ tubulins [45-47]. It was not until the crystal structure of FtsZ from *Methanococcus jannaschii* was determined in 1998 that the similarity between tubulin and FtsZ was fully appreciated [15, 48]. Despite limited (10-18%) sequence similarity [49], FtsZ and tubulin share a common fold, comprised of two domains linked by an α -helix [50]. Conserved residues between the two proteins map to the nucleotide-binding domain and a region involved in protofilament formation in tubulin. Consistent with these observations, like tubulin, FtsZ GTP hydrolysis is self-activated, with the active site being formed by interaction of two monomers [38]. FtsZ subunits polymerize in the presence of GTP into straight, 5 nm-wide protofilaments, while the subsequent hydrolysis of GTP results in the filaments adopting a curved conformation. Just as microtubule stability is controlled by microtubule associated proteins (MAPs), assembly of FtsZ is influenced *in vivo* by proteins such as FtsA, ZipA and ZapA [51-54]. Taken together, the similarities between both protein families suggest that FtsZ may be a prokaryotic cytoskeletal protein homologue of tubulin [49, 55, 56] and support the hypothesis that ancient FtsZ might have evolved into tubulin [49, 57, 58]. While tubulin and FtsZ share some common features, the two proteins also differ in important ways. While FtsZ subunits

are all identical, microtubules are formed from non-identical paired subunits (α - and β -tubulin). As shown in Fig. 4, the two Mtb FtsZ subunits (A and B) in the crystallographic asymmetric unit associate laterally, rather than longitudinally like tubulin protofilaments (Fig. 4C), to form an arc-shaped dimer [16]. A model for a Mtb FtsZ spiral filament is shown in Fig. 4D.

Given the importance of FtsZ assembly in cell division, compounds that interfere with FtsZ function have good potential as novel antibacterial agents. Because of structural and functional homology between FtsZ and tubulin, compounds that are known to affect the assembly of tubulin into microtubules, provide a starting point for targeting FtsZ assembly. While the structures of tubulin and FtsZ are similar, the fact that FtsZ and tubulin have limited sequence homology (<20% identity) at the protein level, affords the opportunity to discover FtsZ-specific compounds with limited cytotoxicity to eukaryotic cells. Therefore, FtsZ can be considered as an attractive target for the development of agents with selective inhibitory activity against bacterial pathogens. In addition, investigating the effects of tubulin inhibitors on FtsZ assembly should also provide important information for FtsZ structure and function.

COMPOUNDS TARGETING *ESCHERICHIA COLI* FTSZ

Viriditoxin

Using a high-throughput FtsZT65C-fluorescein polymerization assay [60], Wang *et al.* [61] screened more than 100,000 microbial fermentation broths and plant extracts and discovered a small molecule, viriditoxin (Fig. 5), which blocked *E. coli* FtsZ polymerization (IC₅₀ 8.2 μ g/ml) and inhibited GTP hydrolysis (IC₅₀ 7.0 μ g/ml). Morphological assays with a specific *E. coli* strain (SOS-, Sula-) showed that viriditoxin caused filamentation, and that the filaments were not formed as a result of DNA damage. The increased MIC resulting from the induction of FtsZ expression provided solid evidence that viriditoxin interacts with FtsZ. Furthermore, viriditoxin exhibited broad-spectrum antibacterial activity against many clinically relevant Gram-positive pathogens, which indicated a high functional conservation of FtsZ in these clinically important species. Presumably, the structure of the FtsZ molecule is highly conserved in the viriditoxin-binding site, a fact that may limit the ability of FtsZ to develop resistance to this drug.

Zantrins

After a high throughput protein based chemical screening of 18,320 compounds, Margalit *et al.* [11] reported the identification of five structurally diverse molecules, named Zantrins (Fig. 6), that inhibit GTPase activity of *E. coli* FtsZ at IC₅₀ values below 50 μ M. Results from electron microscopy and quantification of effects of Zantrins on steady state FtsZ polymer mass and structure, indicated that Zantrins inhibit FtsZ GTPase either by destabilizing the FtsZ protofilaments (Z1 and Z4) or by inducing filament hyperstability (Z2, Z3 and Z5). Margalit *et al.* [11] proposed that Zantrins that destabilize the FtsZ polymer may bind at a site between the FtsZ subunits such that the T7 synergy loop in one FtsZ monomer fails to make optimum contact with the GTP bound to loops T1-T6 in the neighboring monomer, an

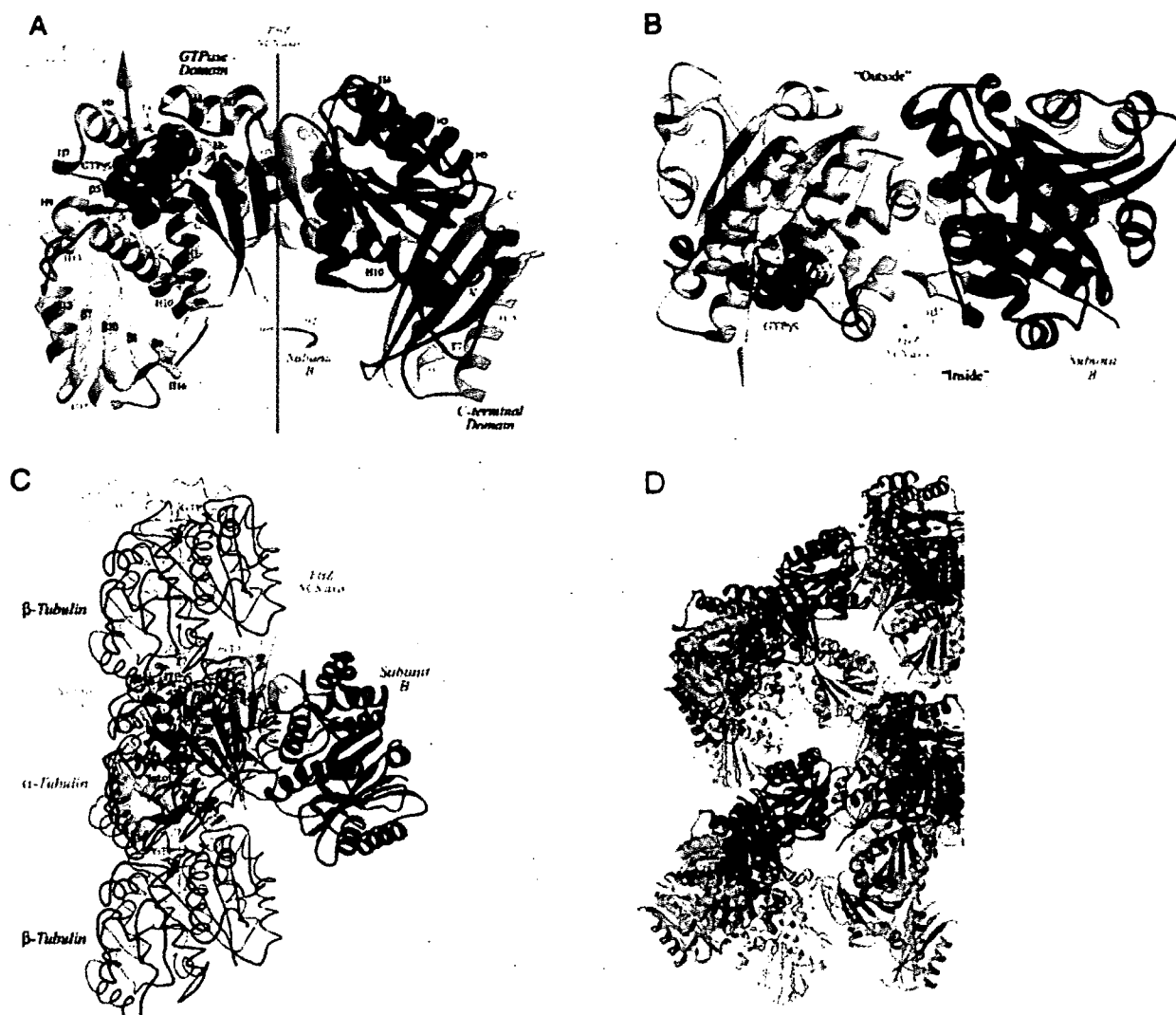


Fig. (4). (A) The GTP γ S complex (Mtb FtsZ, subunit A, yellow; subunit B, brown) is viewed from the “inside” of a corresponding microtubule. GTP γ S bound to the subunit A active site is shown as a space-filling model (nitrogen, blue; oxygen, red; phosphorous, yellow-green; carbon, grey; sulfur, purple). The switch elements at the subunit interface within the dimer are highlighted in light blue. The active sites are lavender. The two Mtb FtsZ subunits are related by a $\sim 92^\circ$ rotation about the vertical axis (grey); this axis is canted by $\sim 50^\circ$ from the $\alpha\beta$ -tubulin protofilament axis (light green), drawn with the arrowhead pointing in the (+)-direction. (B) Rotated by 90° about a horizontal axis (from the top in A), to better illustrate the dimer interface. (C) Comparison of the Mtb FtsZ dimer with the $\alpha\beta$ -tubulin protofilament (PDB entry 1jff) [59]. Subunit A was aligned with the exchangeable (E) α -tubulin subunit (blue), which contains GDP (green) in its active site and a bound Taxol (purple) molecule. The two adjacent non-exchangeable (N) β -tubulin subunits (black) in the protofilament contain GTP (red). The protofilament axis is vertical. (D) A model for an FtsZ spiral filament. A, Twenty-four Mtb FtsZ subunits forming a right-handed spiral are shown in this stereoview. The B (brown) and A (yellow) subunits alternate.

Reprinted from [16] *J. Mol. Biol.*, 342, (3), Leung, A. K. W.; White, E. L.; Ross, L. J.; Reynolds, R. C.; DeVito, J. A.; Borhani, D. W.. Structure of *Mycobacterium tuberculosis* FtsZ Reveals Unexpected, G Protein-like Conformational Switches, 953-970., Copyright (2004), with permission from Elsevier.

interaction essential for polymerization and for stimulating nucleotide hydrolysis [62, 63]. They also proposed that the stabilizing Zantrins could inhibit FtsZ depolymerization by opposing the movement of the T3 switch loop that has been proposed to cause a bend in the filament upon GTP hydrolysis. In support of this suggestion, results from immunofluorescence microscopy demonstrate that Zantrins perturb FtsZ ring assembly in *E. coli* cells. Interestingly, Zantrins Z3 and Z5, which stabilize FtsZ polymers *in vitro*, caused a significant reduction in Z ring assembly in *E. coli*. Z3 and Z5

may disrupt FtsZ's recruitment of other stabilizing factors, such as ZipA and FtsA, to the septum. Zantrins have also been tested against FtsZ from Mtb. The majority of Zantrins inhibited Mtb FtsZ GTPase with IC₅₀ values up to one order of magnitude higher than the corresponding values against *E. coli* FtsZ. Zantrins have also been observed to cause lethality to a variety of bacteria in broth cultures, including antibiotic-resistant and virulent pathogens, further supporting the hypothesis that FtsZ is a good target for the development of new broad-spectrum antibacterial agents.

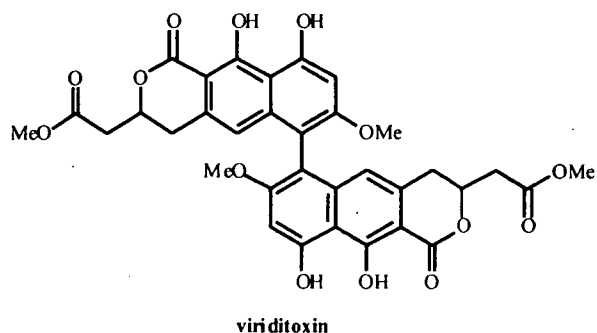


Fig. (5). Chemical structure of viriditoxin.

GTP Analogue BrGTP

Läppchen *et al.* [42] designed a selective *E. coli* FtsZ inhibitor BrGTP (Fig. 7) based on the structure of the natural substrate GTP. Presumably, BrGTP competes with GTP for the binding site on soluble FtsZ. The inhibitory activity of

BrGTP was first demonstrated by electron microscopy which showed that addition of BrGTP resulted in shorter and thinner FtsZ filaments. The inhibitory activity of BrGTP was further characterized by a coupled assay, which allowed simultaneous detection of the extent of polymerization and GTPase activity. The results demonstrated the reversible competitive inhibition of FtsZ by BrGTP. In the GTP concentration range studied, the IC_{50} values depend on the ratio of BrGTP to GTP, which is approximately 1/2 for assembly and 1/1 for GTPase activity, suggesting that both nucleotides bind with equal affinity and that BrGTP-FtsZ is inactive. Interestingly, the addition of a 2-fold excess of BrGTP when FtsZ had fully polymerized resulted in complete FtsZ depolymerization and inhibition of GTPase activity within 5 seconds, indicating that BrGTP could also lead to polymer destabilization by directly replacing GTP/GDP in the polymers. The observation that BrGTP does not inhibit tubulin assembly indicates that there are subtle differences between the GTP binding sites in FtsZ and tubulin.

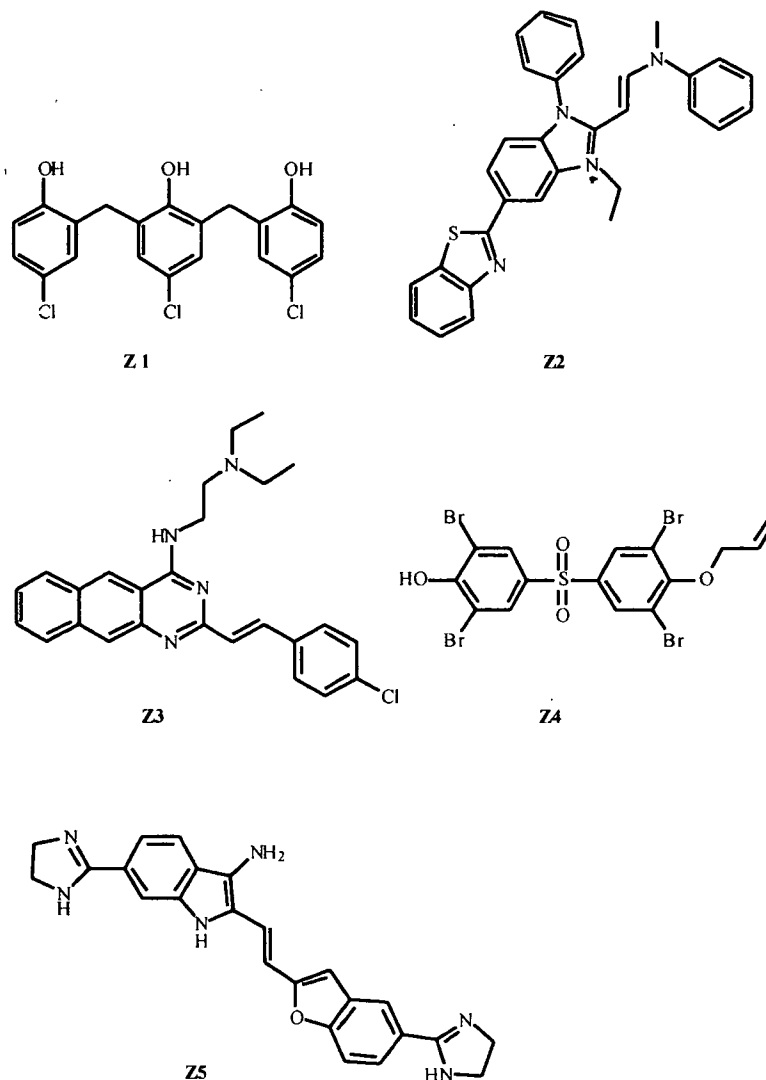


Fig. (6). Chemical structures of Zantrins.

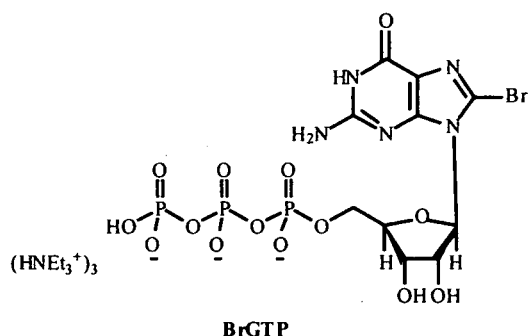


Fig. (7). Chemical structures of BrGTP.

Sanguinarine

Sanguinarine (Fig. 8) a benzophenanthridine alkaloid derived from the rhizomes of *Sanguinaria canadensis*, has a wide range of antimicrobial activity [64]. It is also known to inhibit proliferation of various types of cancer cells [65, 66] and has been shown to depolymerize microtubules both *in vitro* and in cancer cells [67, 68]. Recently, Beuria *et al.* [69] reported that sanguinarine inhibited cytokinesis in both Gram-positive and Gram-negative bacteria by perturbing Z-ring assembly through FtsZ binding. In both *E. coli* and *B. subtilis* cells, sanguinarine not only reduced the frequency of Z-ring occurrence, but also perturbed the Z-ring morphology, resulting in increased cell length in bacteria. Further *in vitro* experiments demonstrated that sanguinarine was found to bind to FtsZ with a dissociation constant of 18-30 μM . Sanguinarine was shown to reduce the light-scattering caused by FtsZ assembly, to decrease the sedimentable polymeric mass, and to perturb the bundling of FtsZ protofilaments.

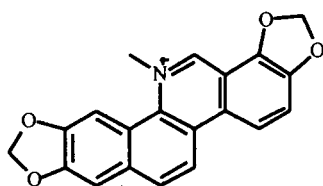


Fig. (8). Chemical structures of sanguinarine.

FtsZ is essential for bacterial cell division and represents an excellent novel target for anti-bacterial drug discovery. Although FtsZ shows a high degree of similarity among bacterial species, there are some important differences between the *E. coli* and Mtb enzymes. Mtb FtsZ shares ~46% amino acid identity with *E. coli* FtsZ, and has been shown to be a markedly slower GTPase *in vitro* [11, 70]. In addition, Mtb FtsZ has some characteristics more reminiscent of its homologue tubulin than the *E. coli* protein [70]. Therefore, compounds targeting *E. coli* FtsZ may not inhibit the Mtb FtsZ or have anti-TB activity.

COMPOUNDS TARGETING MTB FTSZ AS POTENTIAL ANTI-TB AGENTS

Bis-ANS

Bis-ANS (Fig. 9), a well known fluorescent probe for hydrophobic surfaces on proteins, was shown to inhibit tubulin polymerization [71]. In 1998, Yu and Margolin [72] reported the inhibition of *E. Coli* FtsZ assembly by bis-ANS and proposed that bis-ANS inhibited FtsZ polymerization by blocking FtsZ intermolecular hydrophobic interactions. The titration of FtsZ with bis-ANS and *vice versa*, using the same methods that were previously applied to tubulin, suggested that FtsZ has a high affinity bis-ANS binding site as well as multiple low affinity binding sites, with K_d values similar to those of tubulin. The inhibition of bis-ANS binding by GTP binding, and *vice versa*, suggested that the GTP and bis-ANS binding sites overlapped. Subsequently, Nair *et al.* [73] demonstrated that 50 μM bis-ANS significantly reduced the GTPase activity of Mtb FtsZ as well as completely abolished FtsZ polymerization in a light scattering assay. Interestingly, in support of the observed *in vitro* inhibition, Slayden *et al.* [74] demonstrated that bis-ANS inhibited Mtb cell growth ($H37_{Rv}$) with a MIC_{99} value of 1 μM , and also that sub-MIC concentrations of bis-ANS caused filamentation in Mtb. ANS (Fig. 9), a hydrophobic probe similar to bis-ANS, had no inhibitory effect on FtsZ assembly or tubulin assembly, suggesting that FtsZ and tubulin share similar conformational properties and may interact similarly with bis-ANS and ANS [72].

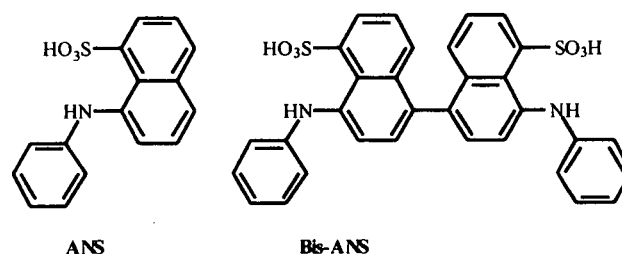
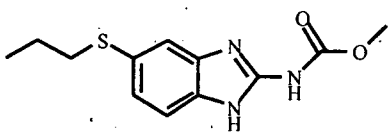
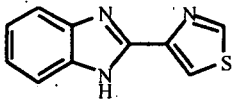


Fig. (9). Chemical structures of ANS and Bis-ANS.

Thiabendazole and Albendazole

Albendazole and thiabendazole (Table 1) are known inhibitors of tubulin polymerization via competitive binding at the same site as colchicine. Importantly, Sarcina and Mullineaux [75] demonstrated that thiabendazole caused cell elongation in *E. coli* and cyanobacteria, a phenotypic response identical to that elicited by disruption of the FtsZ gene in these organisms, suggesting that these tubulin inhibitors may act in a similar manner on the FtsZ gene product as they do on tubulin. They also observed unaffected DNA replication and mobility of thylakoid membrane components accompanied by cell elongation, which indicated that thiabendazole had a specific effect on cell division. Later, Slayden *et al.* [76] determined the MIC_{99} values of thiabendazole and albendazole against Mtb cell growth (Table 1), and studied their effects on bacterial

Table 1. Data for Tubulin Polymerization Inhibitors: Albendazole and Thiabendazole

Compound	MIC ₉₉ (H37Rv)
 Albendazole	16 µg/mL (61 µM)
 Thiabendazole	16 µg/mL (80 µM)

ultrastructure (filamentation) and transcriptional response. The results indicated that thiabendazole and albendazole interfere and delay Mtb cell division processes at inhibitory concentrations. In addition, the fact that these drugs have inhibitory activity provides compelling evidence that the

inhibition of FtsZ polymerization is a novel drug target that warrants further research focus.

2-Alkoxy-carbonylaminopyridines

Investigators at Southern Research Institute [77-79] screened their compound library of 200 2-alkoxy-carbonylaminopyridines, developed to inhibit tubulin polymerization, for the ability to inhibit FtsZ polymerization and for the ability to inhibit growth of Mtb. Using this approach, they identified several compounds with the desired properties. Colchicine, a known tubulin inhibitor, was also included in the study as a reference compound. SRI-3072, SRI-7614, and colchicine inhibited Mtb FtsZ polymerization and GTP hydrolysis in a dose dependant manner (Table 2). SRI-3072 and SRI-7614 were equipotent against susceptible and single-drug-resistant strains of Mtb (Table 3). Importantly, there is a clear correlation between the antibacterial activity of selected compounds (as illustrated by SRI-3072 and SRI-7614) and inhibition of FtsZ polymerization and GTP hydrolysis. Like colchicine, SRI-7614 inhibited polymerization of both FtsZ and tubulin, while SRI-3072 was specific for FtsZ and did not affect the polymerization of tubulin. Furthermore, SRI-3072 reduced the growth of Mtb in mouse-derived macrophages.

Table 2. Results for Inhibition of *M. tuberculosis* H37Rv Growth

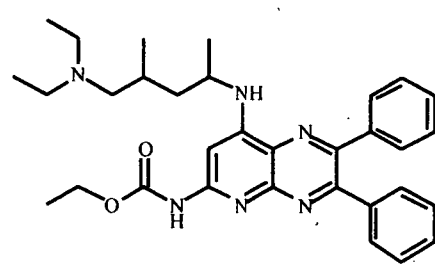
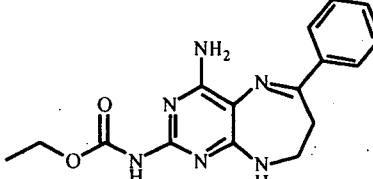
Compound	Structure	MIC ₉₉ (mg/L)	IC ₅₀ (mg/L)	ST (IC ₅₀ : MIC)
SRI-3072		0.15	6.3	42.0
SRI-7614		6.25	>200	>32

Table 3. Inhibitors of FtsZ and Tubulin Polymerization and GTP Hydrolysis

Compounds	<i>M. tuberculosis</i> FtsZ		Bovine brain tubulin
	Polymerization ID ₅₀ (µM)	GTP hydrolysis % inhibition (100 µM)	Polymerization ID ₅₀ (µM)
Colchicine	104 ± 2	35	6.5
SRI-3072	52 ± 12	20	100 (no inhibition)
SRI-7614	60 ± 0	25	4

Taxanes

Taxanes [80, 81], synthesized in our lab, were first screened for inhibitory activity by a real time PCR-based (RT-PCR) assay [81]. These taxanes represent two diverse activities; highly cytotoxic taxoids (i.e., "taxol-like compounds") that stabilize microtubules [82-84] and noncytotoxic (or very weakly cytotoxic) taxane-multidrug-resistance (MDR) reversal agents (TRAs) [85-92] which inhibit the efflux pumps of ATP-binding cassette (ABC) transporters such as P-glycoprotein (P-gp), multidrug resistant protein (MRP-1), and breast cancer resistant protein (BCRP). Screening of 120 taxanes revealed that a number of taxanes exhibited significant anti-TB activity. The antibacterial activity of each compound was confirmed by determining MIC₉₉ values using the conventional microdilution broth assay [81].

In the MIC assay, it was found that SB-RA-2001 [92], bearing a (*E*)-3-(naphth-2-yl)acryloyl (2-NpCH=CHCO) group at the C-13 position possessed very promising anti-TB activity against drug-resistant as well as drug sensitive Mtb strains (MIC₉₉ = 2.5-5 μM; Table 4). SB-RA-2001 [92] was selected as the lead compound for further optimization, and a new library of taxanes was prepared by modification of 10-deacetylbaccatin III (DAB) (Fig. 10 and Scheme 1).

For the FtsZ-binding taxane-based anti-TB agents to be useful as therapeutic drugs, these agents should not be cytotoxic at the concentration required for their antibacterial activity. Accordingly, it is necessary for the agents to distinguish human β tubulin from Mtb FtsZ. It has been shown in the SAR studies of paclitaxel (Taxol, Fig. 11) and taxoids that substitution at the *para*-position of the C-2 benzoate [84, 93] substantially diminishes the binding ability of the analogues. Furthermore, the C-10 position may affect anti-TB activity. Therefore, we synthesized C-2 and C-10 modified SB-RA-2001 (Scheme 1, eq 1) to examine the effects of those modifications on cytotoxicity, FtsZ binding ability, and anti-TB activity. Some C-10 modified SB-RA-2001 analogues show little or no anti-TB activity, while C-2 modification of SB-RA-2001 results in slightly decreased cytotoxicity and does not affect the anti-TB activity.

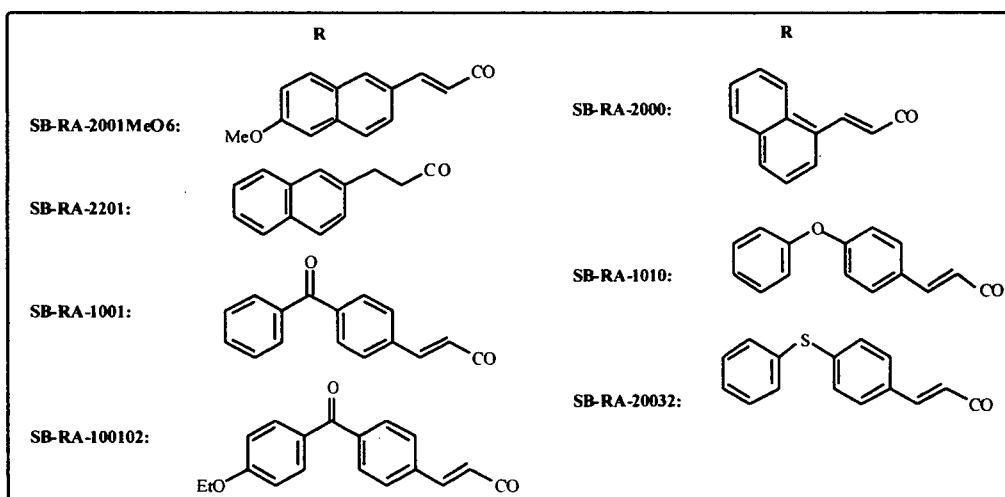
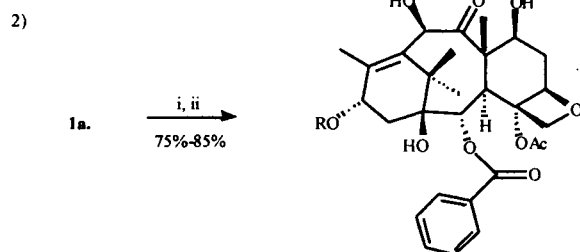
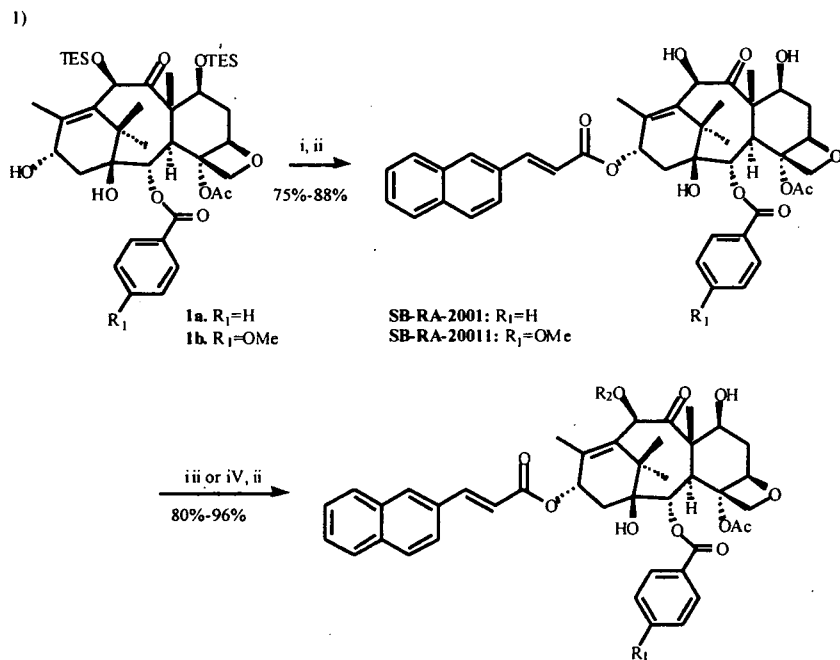
A variety of hydrophobic side chains were appended to the C-13 position of DAB in order to generate a series of SB-RA-2001 analogues (Scheme 1, eq 2). Screening of these compounds revealed several taxanes with activity as good as that of SB-RA-2001 (entries 3, 5, 7, and 8, Table 4).

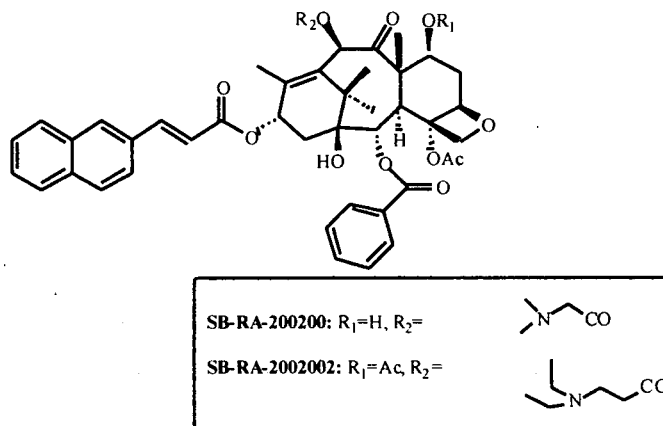
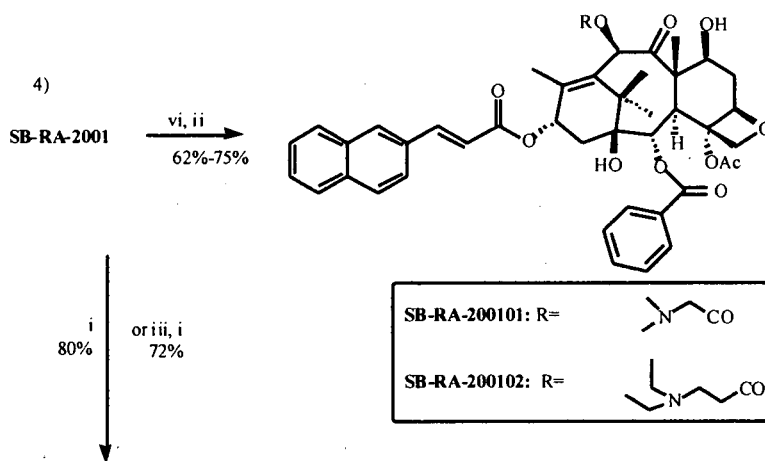
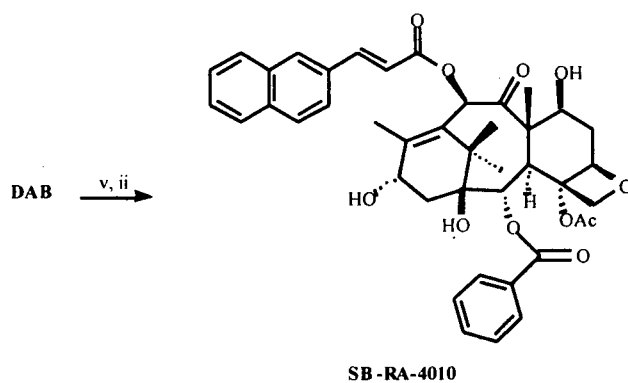
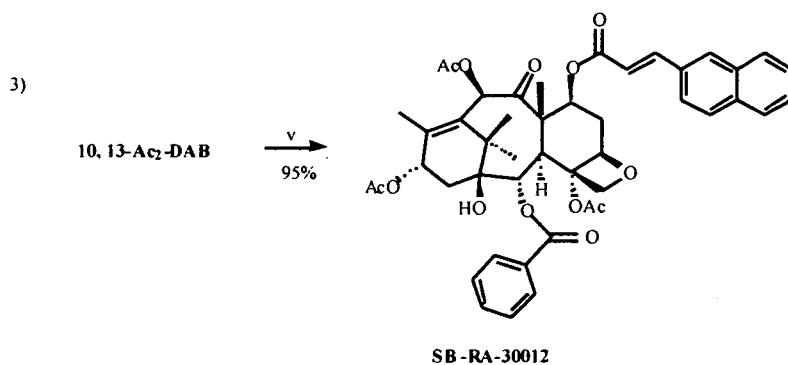
We also examined whether the attachment of the 3-(2-naphthyl)acrylate side chain to the C-13 position is crucial

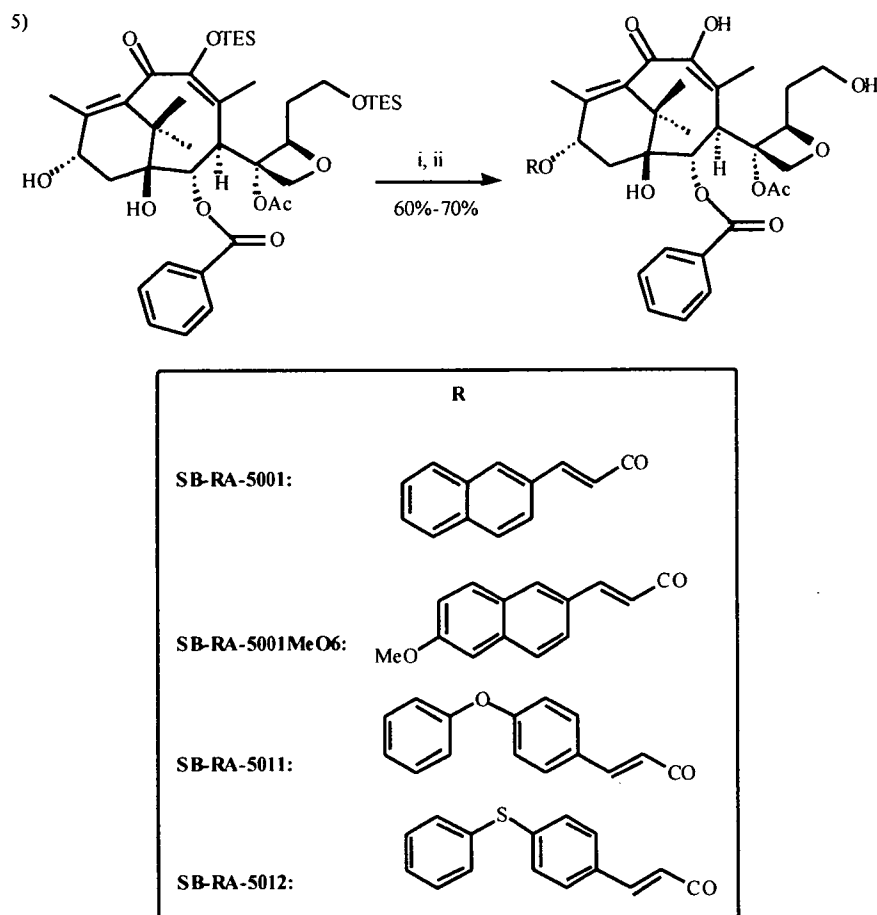
Table 4. Antimicrobial Activities of Taxanes Against Drug-Sensitive and Mutidrug-Resistant *M. tuberculosis*^a

Entry	Taxane	MIC (μM)		Cytotoxicity (IC ₅₀ , μM)	
		<i>M. tuberculosis</i> H37Rv	<i>M. tuberculosis</i> IMCJ946.K2	MCF7	A549
1	Paclitaxel	40	40	0.019	0.028
2	SB-T-0032	5	1.25	0.65	0.65
3	SB-RA-2001	5	2.5	4.5	15.7
4	SB-RA-20011	5	2.5	7.6	14.0
5	SB-RA-2000	5	5	5.4	80
6	SB-RA-1010	10	10	9.3	12.5
7	SB-RA-20032	2.5	2.5	3.4	4.5
8	SB-RA-2001MeO6	5	5	5.3	5.0
9	SB-RA-4010	20	10	14	N.D.
10	SB-RA-200101	10	10	7.0	10.8
11	SB-RA-200102	10	5	3.9	9.6
12	SB-RA-200200	20	5	>20	4.3
13	SB-RA-2002002	10	20	9.4	17.0
14	SB-RA-5001	2.5	1.25	>80	>80
15	SB-RA-5001MeO6	2.5	2.5	>80	>80
16	SB-RA-5011	2.5	1.25	>80	>80
17	SB-RA-5012	2.5	1.25	>80	>80

^a*M. tuberculosis* (Mtb) H37Rv is sensitive to all antibiotics tested. *M. tuberculosis* IMCJ946.K2 is resistant to nine drugs including INH, REF, EB, streptomycin (SM), kanamycin (KM), ethionamid (ETH), *p*-aminosalicylic acid (PAS), cycloserine (CS) and enniomycin (EVM). MCF7 and A549 cells: human breast and non-small cell lung cancer cell lines, respectively. Reprinted with permission from [80] *J. Med. Chem.* 2006, 49, (2), 463-466. Copyright 2006 American Chemical Society.







Scheme 1. Synthesis of taxane-based anti-TB agents^a

^aReagents and conditions: (i) RCOOH, DIC, DMAP, CH₂Cl₂; (ii) HF/Pyridine, CH₃CN/Pyridine, room temperature, overnight; (iii) CeCl₃, acid anhydride, THF, room temperature, 4h-6h; (iv) TESCl, imidazole, room temperature; Acid chloride, LiHMDS, THF, -40°C; (v) RCOOH, EDC, DMAP, CH₂Cl₂, room temperature. Reprinted with permission from [80] *J. Med. Chem.* **2006**, *49*, (2), 463-466. Copyright 2006 American Chemical Society

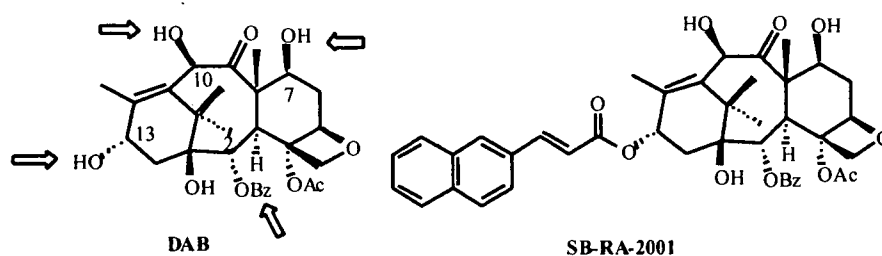


Fig. (10). Chemical structures of DAB and SB-RA-2001. Reprinted with permission from [80] *J. Med. Chem.* **2006**, *49*, (2), 463-466. Copyright 2006 American Chemical Society.

for the anti-TB activity of the SB-RA-2001 series via interaction with FtsZ. Accordingly, we attached the same side chain moiety to the C-7 and C-10 position to see the effects of these changes on the potency and profile of the resulting taxanes (Scheme 1, eq 3). In fact, the 10 modified analogue SB-RA-4010 showed only slightly reduced anti-TB activity (entry 9, Table 4).

In addition to the above modifications, we also introduced functionalities to improve the water solubility of these TRAs. Thus, *N,N*-dimethylglycine and *N,N*-diethyl- β -alanine esters were introduced to SB-RA-2001 as a pendant group at the C-7 or C-10 position (Scheme 1, eq 4). This modification caused only minor reduction in the anti-TB activity of these analogues (SB-RA-200101, SB-RA-200102, SB-RA-

200200, and SB-RA-2002002) as compared with SB-RA-2001 (entries 3, 10, 11, 12, and 13, Table 4).

Although SB-RA-2001 is certainly an excellent lead compound for optimization, it will be even better if a noncytotoxic lead compound, which does not bind to microtubules at all, is identified. Recently, we have been investigating a novel antiangiogenic taxoid (IDN5390) [94, 95], which bears a C-secobaccatin (i.e., C-ring-opened baccatin) skeleton and is much less cytotoxic than paclitaxel. Accordingly, we prepared the C-seco analogue of SB-RA-2001, i.e., SB-RA-5001 (Scheme 1, eq 5). Three analogues of SB-RA-5001 (Fig. 12) were also prepared and assayed for their anti-TB activity and cytotoxicity. Significantly, SB-RA-5001 series compounds (entries 14-17, Table 4) possessed potent anti-TB activity (MIC 1.25-2.5 μM) against drug sensitive and drug-resistant MTB strains without appreciable cytotoxicity ($\text{IC}_{50} > 80 \mu\text{M}$).

As Table 4 shows, paclitaxel, SB-T-0032 (Fig. 11), SB-RA-2001 and its congeners were assayed for their growth inhibitory activity against drug-sensitive Mtb strain (H37Rv) and a multi-drug-resistant strain (IMCJ946K2), cultured from clinical isolates of MDR-TB. The Mtb strain IMCJ 946K2 is associated with nosocomial outbreaks in Japan and is resistant to all the clinically prescribed anti-TB drugs used in Japan (9 drugs; see Table 4 legend).

Paclitaxel (Fig. 11), a microtubule-stabilizing anticancer agent, exhibits modest antibacterial activity against both Mtb strains (MIC 40 μM), but its cytotoxicity against human cancer cell lines (a benchmark for activity against human

host cells) is 3 orders of magnitude more potent (IC_{50} 0.019-0.028 μM ; entry 1, Table 4). These data clearly indicate that paclitaxel is highly specific for microtubules. SB-T-0032 (Fig. 11) exhibits one order of magnitude higher antibacterial potency and 20-30 times reduced cytotoxicity compared to paclitaxel. Since it is likely that the IC_{99} values would be at least 10 times larger than the IC_{50} values (as the former measures complete cell growth inhibition while the latter only measures 50% inhibition), it appears that SB-T-0032 has comparable affinities to microtubules and FtsZ (entry 2, Table 4). SB-RA-2001 and its congeners derived from DAB (entries 3-13, Table 4) are clearly much less cytotoxic than paclitaxel (200-1000 times less toxic) and SB-T-0032, while keeping the same level of antibacterial activity to that of SB-T-0032. These TRAs appear to have higher specificity to FtsZ than microtubules. As entries 14-17, Table 4 clearly indicated, C-seco-TRAs are noncytotoxic so far at the upper limit of solubility and detection, while keeping the MIC values of 1.25-2.5 μM against drug-resistant and drug-sensitive Mtb strains. Thus, we have now discovered noncytotoxic taxane lead compounds to develop a novel class of anti-TB agents. The specificity of these novel taxanes to microtubules as compared to FtsZ appears to have been completely reversed through systematic rational drug design. Moreover, we observed that the treatment of Mtb cells with SB-RA-5001 at the MIC caused filamentation and prolongation of the cells (Fig. 13), a phenotypic response to FtsZ inactivation. In addition, a preliminary study on the effect of TRA SB-RA-5001 on FtsZ polymerization and depolymerization using the standard light scattering assay

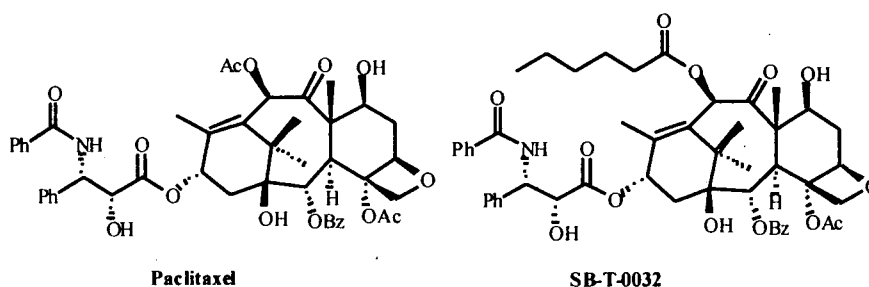


Fig. (11). Chemical structures of paclitaxel and SB-T-0032.

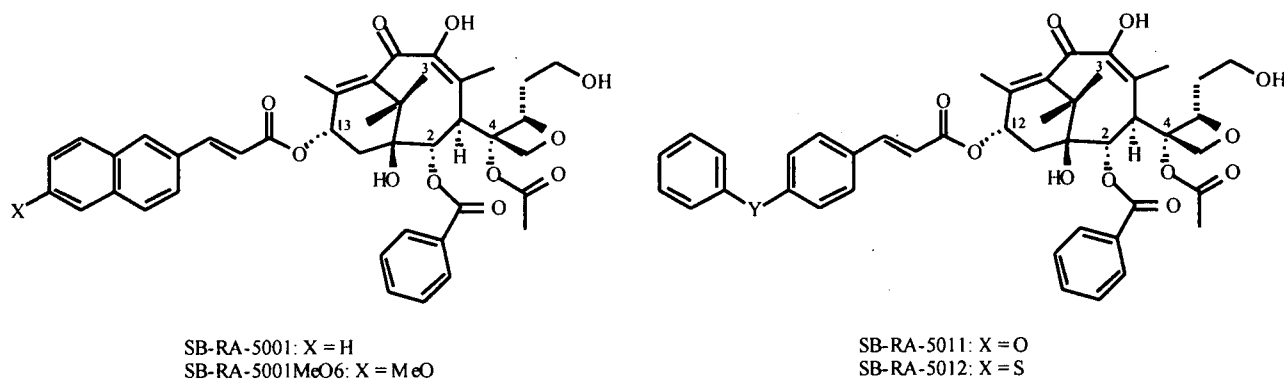


Fig. (12). Chemical structures of highly promising noncytotoxic anti-TB taxane leads derived from C-seco-baccatin.



Fig. (13). Electron micrographs of Mtb cells before (Control) and after treatment with SB-RA-20018 and SB-RA-5001. Reprinted with permission from [80] *J. Med. Chem.* 2006, 49, (2), 463-466. Copyright 2006 American Chemical Society.

demonstrated a dose-dependent stabilization of FtsZ against depolymerization.

CONCLUSION

Multi-drug resistant Mtb is a major worldwide health problem. Therefore, it is critical to develop new antibiotics with novel modes of action to overcome this emerging resistance problem. FtsZ, a tubulin-like GTPase, plays an essential role in bacterial cell division, and is present in almost all eubacteria and archaea. Inhibitors of the GTP-dependent polymerization of FtsZ are expected to result in a new class of antibacterial agents.

The strong structural homology between FtsZ and tubulin raises the possibility that some of tubulin inhibitors could affect bacterial cell division. The search for a suitable lead compound was greatly facilitated by screening libraries of tubulin inhibitors. The fact that the protein sequence homology between FtsZ and tubulin is low (<20% identity) strongly indicates an excellent possibility in discovering FtsZ specific agents that are non-cytotoxic to eukaryotic cells. Recently, a number of FtsZ inhibitors have been reported. Some of them have been observed to perturb Z ring assembly, and cause bacterial lethality, confirming the hypothesis that FtsZ is a sensitive target for anti-TB drug discovery. However, much remains to be done to exploit FtsZ as a new target. Structural and kinetic analysis of compounds binding to FtsZ, determining the mechanism of drug action and evaluating structure relationships of active compounds are all critical aspects of the rational drug discovery process, which will facilitate the further optimization of chemical leads into specific FtsZ inhibitors with high affinity.

ACKNOWLEDGMENT

The authors gratefully acknowledge the grant support from the National Institutes of Health and the Japan Health Science Foundation. Generous support from Indena, SpA, Italy is also appreciated.

ABBREVIATIONS

ABC = ATP-binding cassette

AIDS	=	Acquired Immune Deficiency Syndrome
ANS	=	1-Anilino-naphthalene-8-sulfonate
BCRP	=	Breast cancer resistant protein
Bis-ANS	=	4,4'-Dianilino-1,1'-binaphthyl-5,5'-sulfonate
BrGTP	=	8-bromoguanosine 5'-triphosphate
DAB	=	10-deacetyl-baccatin III
DNA	=	Deoxyribonucleic acid
<i>E. Coli</i>	=	<i>Escherichia coli</i>
HIV	=	Human immunodeficiency virus
IC ₅₀	=	Concentration of compound that inhibits the growth of cells by 50%
IC ₉₉	=	Concentration of compound that inhibits the growth of cells by 99%
MAPs	=	Microtubule associated proteins
MDR	=	Multi-drug resistant
MIC	=	Minimum inhibitory concentration
MRP	=	Multidrug resistant protein
Mtb	=	<i>Mycobacterium tuberculosis</i>
P-gp	=	P-glycoprotein
FRAP	=	Fluorescence recovery after photobleaching
Fts	=	Filament-forming temperature-sensitive genes
GDP	=	Guanosine-5'-diphosphate
GFP	=	Green fluorescent protein
GTP	=	Guanosine-5'-triphosphate
RT-PCR	=	Real-time polymerase chain reaction
SAR	=	Structure activity relationship
TRAs	=	Taxane-multidrug-resistance reversal agents

WHO = World Health Organization

REFERENCES

- [1] Sudre, P.; ten Dam, G.; Kochi, A. Tuberculosis: a global overview of the situation today. *B. World Health Organ.* **1992**, *70* (2), 149-59.
- [2] Bloom, B. R.; Murray, C. J. Tuberculosis: commentary on a reemergent killer. *Science* **1992**, *257* (5073), 1055-64.
- [3] W.R. Global Tuberculosis Control. **2001**.
- [4] Raviglione, M. C. Issues facing TB control (7). Multiple drug-resistant tuberculosis. *Scot. Med. J.* **2000**, *45* (5 Suppl), 52-5; discussion 56.
- [5] Kochi, A. The global tuberculosis situation and the new control strategy of the World Health Organization. *Tubercle* **1991**, *72* (1), 1-6.
- [6] Gupta, R.; Kim, J. Y.; Espinal, M. A.; Caudron, J.-M.; Pecoul, B.; Farmer, P. E.; Raviglione, M. C. Policy forum: Public health: Responding to market failures in tuberculosis control. *Science (Washington, DC, U.S.)* **2001**, *293* (5532), 1049-1051.
- [7] Tuberculosis Fact sheet. *MSF CAMPAIGN FOR ACCESS TO ESSENTIAL MEDICINES* **2005**.
- [8] Kreuter, M.; Langer, C.; Kerkhoff, C.; Reddanna, P.; Kania, A. L.; Maddika, S.; Chlichlia, K.; Bui, T. N.; Los, M. Stroke, myocardial infarction, acute and chronic inflammatory diseases: Caspases and other apoptotic molecules as targets for drug development. *Archivum Immunologiae et Therapiae Experimentalis* **2004**, *52* (3), 141-155.
- [9] Falchetti, M. L.; Pallini, R.; Levi, A. Telomerase and cancer: A promising target. *Am. J. Cancer (Auckland, New Zealand)* **2004**, *3* (1), 1-11.
- [10] Fingar, D. C.; Richardson, C. J.; Tee, A. R.; Cheatham, L.; Tsou, C.; Blenis, J. mTOR controls cell cycle progression through its cell growth effectors S6K1 and 4E-BP1/eukaryotic translation initiation factor 4E. *Mol. Cell. Biol.* **2004**, *24* (1), 200-216.
- [11] Margalit, D. N.; Romberg, L.; Mets, R. B.; Hebert, A. M.; Mitchison, T. J.; Kirschner, M. W.; RayChaudhuri, D. Targeting cell division: Small-molecule inhibitors of FtsZ GTPase perturb cytokinetic ring assembly and induce bacterial lethality. *Proc. Natl. Acad. Sci. USA* **2004**, *101* (38), 13969.
- [12] Hirota, Y.; Ryter, A.; Jacob, F. Thermosensitive mutants of *E. coli* affected in the processes of DNA synthesis and cellular division. *Cold Spring Harbor Symp. Quant. Biol.* **1968**, *33*, 677-93.
- [13] Van De Putte, P.; Van, D.; Roersch, A. The Selection of Mutants of *Escherichia Coli* with Impaired Cell Division at Elevated Temperature. *Mutat. Res.* **1964**, *106*, 121-8.
- [14] Bi, E.; Lutkenhaus, J. FtsZ ring structure associated with division in *Escherichia coli*. *Nature (London, U. K.)* **1991**, *354* (6349), 161-164.
- [15] Goehring, N. W.; Beckwith, J. Diverse paths to midcell: assembly of the bacterial cell division machinery. *Curr. Biol.* **2005**, *15* (13), R514-R526.
- [16] Leung, A. K. W.; White, E. L.; Ross, L. J.; Reynolds, R. C.; DeVito, J. A.; Borhani, D. W. Structure of *Mycobacterium tuberculosis* FtsZ Reveals Unexpected, G Protein-like Conformational Switches. *J. Mol. Biol.* **2004**, *342* (3), 953-970.
- [17] Thanedar, S.; Margolin, W. FtsZ Exhibits Rapid Movement and Oscillation Waves in Helix-like Patterns in *Escherichia coli*. *Curr. Biol.* **2004**, *14* (13), 1167-1173.
- [18] Ben-Yehuda, S.; Losick, R. Asymmetric cell division in *B. subtilis* involves a spiral-like intermediate of the cytokinetic protein FtsZ. *Cell (Cambridge, MA, U. S.)* **2002**, *109* (2), 257-266.
- [19] Moller-Jensen, J.; Loewe, J. Increasing complexity of the bacterial cytoskeleton. *Curr. Opin. Cell Biol.* **2005**, *17* (1), 75-81.
- [20] Errington, J.; Daniel, R. A.; Scheffers, D.-J. Cytokinesis in bacteria. *Microbiol. Mol. Biol. R.* **2003**, *67* (1), 52-65.
- [21] Lu, C.; Stricker, J.; Erickson, H. P. FtsZ from *Escherichia coli*, *Azotobacter vinelandii*, and *Thermotoga maritima*-quantitation, GTP hydrolysis, and assembly. *Cell Motil. Cytoskel.* **1998**, *40* (1), 71-86.
- [22] Stricker, J.; Maddox, P.; Salmon, E. D.; Erickson, H. P. Rapid assembly dynamics of the *Escherichia coli* FtsZ-ring demonstrated by fluorescence recovery after photobleaching. *Proc. Natl. Acad. Sci. USA* **2002**, *99* (5), 3171-3175.
- [23] Weiss, D. S. Bacterial cell division and the septal ring. *Mol. Microbiol.* **2004**, *54* (3), 588-597.
- [24] Romberg, L.; Levin, P. A. Assembly dynamics of the bacterial cell division protein FtsZ: Poised at the edge of stability. *Annu. Rev. Microbiol.* **2003**, *57*, 125-154.
- [25] Mingorance, J.; Tadros, M.; Vicente, M.; Gonzalez, J. M.; Rivas, G.; Velez, M. Visualization of Single *Escherichia coli* FtsZ Filament Dynamics with Atomic Force Microscopy. *J. Biol. Chem.* **2005**, *280* (21), 20909-20914.
- [26] Rajagopalan, M.; Atkinson, M. A. L.; Lofton, H.; Chauhan, A.; Madiraju, M. V. Mutations in the GTP-binding and synergy loop domains of *Mycobacterium tuberculosis* ftsZ compromise its function *in vitro* and *in vivo*. *Biochem. Biophys. Res. Commun.* **2005**, *331* (4), 1171-1177.
- [27] Chen, Y.; Bjornson, K.; Redick, S. D.; Erickson, H. P. A rapid fluorescence assay for FtsZ assembly indicates cooperative assembly with a dimer nucleus. *Biophys. J.* **2005**, *88* (1), 505-514.
- [28] Gupta, P.; Anand, S. P.; Srinivasan, R.; Rajeswari, H.; Indi, S.; Ajitkumar, P. The C-terminally truncated mtFtsZ-DC169 mutant of *Mycobacterium tuberculosis* FtsZ shows GTPase and GTP-induced, GTP-specific polymerization activities *in vitro*. *Microbiology (Reading, U. K.)* **2004**, *150*(12), 3906-3908.
- [29] Oliva, M. A.; Cordell, S. C.; Loewe, J. Structural insights into FtsZ protofilament formation. *Nat. Struct. Mol. Biol.* **2004**, *11* (12), 1243-1250.
- [30] Marrington, R.; Small, E.; Rodger, A.; Dafforn, T. R.; Addinall, S. G. FtsZ Fiber Bundling Is Triggered by a Conformational Change in Bound GTP. *J. Biol. Chem.* **2004**, *279* (47), 48821-48829.
- [31] Huecas, S.; Andreu, J. M. Polymerization of nucleotide-free, GDP- and GTP-bound cell division protein FtsZ: GDP makes the difference. *FEBS Lett.* **2004**, *569* (1-3), 43-48.
- [32] Anand, S. P.; Rajeswari, H.; Gupta, P.; Srinivasan, R.; Indi, S.; Ajitkumar, P. A C-terminal deletion mutant of *Mycobacterium tuberculosis* FtsZ shows fast polymerization *in vitro*. *Microbiology (Reading, U. K.)* **2004**, *150* (5), 1119-1121.
- [33] Romberg, L.; Mitchison, T. J. Rate-Limiting Guanosine 5'-Triphosphate Hydrolysis during Nucleotide Turnover by FtsZ, a Prokaryotic Tubulin Homologue Involved in Bacterial Cell Division. *Biochemistry* **2004**, *43* (1), 282-288.
- [34] Huecas, S.; Andreu, J. M. Energetics of the Cooperative Assembly of Cell Division Protein FtsZ and the Nucleotide Hydrolysis Switch. *J. Biol. Chem.* **2003**, *278* (46), 46146-46154.
- [35] Small, E.; Addinall, S. G. Dynamic FtsZ polymerization is sensitive to the GTP to GDP ratio and can be maintained at steady state using a GTP-regeneration system. *Microbiology (Reading, U. K.)* **2003**, *149* (8), 2235-2242.
- [36] Scheffers, D.-J.; Driessen, A. J. M. Immediate GTP hydrolysis upon FtsZ polymerization. *Mol. Microbiol.* **2002**, *43* (6), 1517-1521.
- [37] Mukherjee, A.; Lutkenhaus, J. Dynamic assembly of FtsZ regulated by GTP hydrolysis. *EMBO J.* **1998**, *17* (2), 462-469.
- [38] Scheffers, D. J.; Driessen, A. J. M. The polymerization mechanism of the bacterial cell division protein FtsZ. *FEBS Lett.* **2001**, *506* (1), 6-10.
- [39] Mukherjee, A.; Dai, K.; Lutkenhaus, J. *Escherichia coli* cell division protein FtsZ is a guanine nucleotide binding protein. *Proc. Natl. Acad. Sci. USA* **1993**, *90* (3), 1053-7.
- [40] Mingorance, J.; Rueda, S.; Gomez-Puertas, P.; Valencia, A.; Vicente, M. *Escherichia coli* FtsZ polymers contain mostly GTP and have a high nucleotide turnover. *Mol. Microbiol.* **2001**, *41* (1), 83-91.
- [41] Gonzalez, J. M.; Jimenez, M.; Velez, M.; Mingorance, J.; Andreu, J. M.; Vicente, M.; Rivas, G. Essential Cell Division Protein FtsZ Assembles into One Monomer-thick Ribbons under Conditions Resembling the Crowded Intracellular Environment. *J. Biol. Chem.* **2003**, *278* (39), 37664-37671.
- [42] Läppchen, T.; Hartog, A. F.; Pinas, V. A.; Koomen, G.-J.; Den Blaauwen, T. GTP Analogue Inhibits Polymerization and GTPase Activity of the Bacterial Protein FtsZ without Affecting Its Eukaryotic Homologue Tubulin. *Biochemistry* **2005**, *44* (21), 7879-7884.
- [43] Lu, C.; Reedy, M.; Erickson, H. P. Straight and curved conformations of FtsZ are regulated by GTP hydrolysis. *J. Bacteriol.* **2000**, *182* (1), 164-170.
- [44] Ryan, K. R.; Shapiro, L. Temporal and spatial regulation in prokaryotic cell cycle progression and development. *Annu. Rev. Biochem.* **2003**, *72*, 367-394.

- [45] Erickson, H. P. FtsZ, a tubulin homolog in prokaryote cell division. *Trends Cell Biol.* **1997**, *7* (9), 362-367.
- [46] RayChaudhuri, D.; Park, J. T. Escherichia coli cell-division gene *ftsZ* encodes a novel GTP-binding protein. *Nature (London, U. K.)* **1992**, *359* (6392), 251-254.
- [47] de Boer, P.; Crossley, R.; Rothfield, L. The essential bacterial cell-division protein FtsZ is a GTPase. *Nature* **1992**, *359* (6392), 254-256.
- [48] Lowe, J.; Amos, L. A. Crystal structure of the bacterial cell-division protein FtsZ. *Nature (London, U. K.)* **1998**, *391* (6663), 203-206.
- [49] de Pereda, J. M.; Leynadier, D.; Evangelio, J. A.; Chacon, P.; Andreu, J. M. Tubulin secondary structure analysis, limited proteolysis sites, and homology to FtsZ. *Biochemistry* **1996**, *35* (45), 14203-14215.
- [50] Nogales, E.; Downing, K. H.; Amos, L. A.; Lowe, J. Tubulin and FtsZ form a distinct family of GTPases. *Nat. Struct. Biol.* **1998**, *5* (6), 451-458.
- [51] Amos, L. A.; Van den Ent, F.; Loewe, J. Structural/functional homology between the bacterial and eukaryotic cytoskeletons. *Curr. Opin. Cell Biol.* **2004**, *16* (1), 24-31.
- [52] Rueda, S.; Vicente, M.; Mingorance, J. Concentration and assembly of the division ring proteins FtsZ, FtsA, and ZipA during the Escherichia coli cell cycle. *J. Bacteriol.* **2003**, *185* (11), 3344-3351.
- [53] Pichoff, S.; Lutkenhaus, J. Unique and overlapping roles for ZipA and FtsA in septal ring assembly in Escherichia coli. *EMBO J.* **2002**, *21* (4), 685-693.
- [54] Geissler, B.; Elraheb, D.; Margolin, W. A gain-of-function mutation in *ftsA* bypasses the requirement for the essential cell division gene *zipA* in Escherichia coli. *Proc. Natl. Acad. Sci. USA* **2003**, *100* (7), 4197-4202.
- [55] Erickson, H. P. FtsZ, a prokaryotic homolog of tubulin? *Cell (Cambridge, MA, U. S.)* **1995**, *80* (3), 367-70.
- [56] Vicente, M.; Errington, J. Structure, function and controls in microbial division. *Mol. Microbiol.* **1996**, *20* (1), 1-7.
- [57] Erickson, H. P.; Taylor, D. W.; Taylor, K. A.; Bramhill, D. Bacterial cell division protein FtsZ assembles into protofilament sheets and minirings, structural homologs of tubulin polymers. *Proc. Natl. Acad. Sci. USA* **1996**, *93* (1), 519-23.
- [58] Margolin, W.; Wang, R.; Kumar, M. Isolation of an *ftsZ* homolog from the archaeobacterium Halobacterium salinarium: implications for the evolution of FtsZ and tubulin. *J. Bacteriol.* **1996**, *178* (5), 1320-7.
- [59] Lowe, J.; Li, H.; Downing, K. H.; Nogales, E. Refined structure of alpha beta-tubulin at 3.5 Å resolution. *J. Mol. Biol.* **2001**, *313* (5), 1045-57.
- [60] Trusca, D.; Bramhill, D. Fluorescent assay for polymerization of purified bacterial FtsZ cell-division protein. *Anal. Biochem.* **2002**, *307*, (2), 322-329.
- [61] Wang, J.; Galgoci, A.; Kodali, S.; Herath, K. B.; Jayasuriya, H.; Dorso, K.; Vicente, F.; Gonzalez, A.; Cully, D.; Bramhill, D.; Singh, S. Discovery of a small molecule that inhibits cell division by blocking FtsZ, a novel therapeutic target of antibiotics. *J. Biol. Chem.* **2003**, *278* (45), 44424-44428.
- [62] Lowe, J.; Amos, L. A. Tubulin-like protofilaments in Ca²⁺-induced FtsZ sheets. *EMBO J.* **1999**, *18* (9), 2364-71.
- [63] Scheffers, D.-J.; de Wit, J. G.; den Blaauwen, T.; Driessen, A. J. M. GTP Hydrolysis of Cell Division Protein FtsZ: Evidence that the Active Site Is Formed by the Association of Monomers. *Biochemistry* **2002**, *41* (2), 521-529.
- [64] Godowski, K. C. Antimicrobial action of sanguinarine. *J. Clin. Dent.* **1989**, *1* (4), 96-101.
- [65] Adhami, V. M.; Aziz, M. H.; Reagan-Shaw, S. R.; Nihal, M.; Mukhtar, H.; Ahmad, N. Sanguinarine causes cell cycle blockade and apoptosis of human prostate carcinoma cells via modulation of cyclin kinase inhibitor-cyclin-cyclin-dependent kinase machinery. *Mol. Cancer Ther.* **2004**, *3* (8), 933-940.
- [66] Ahmad, N.; Gupta, S.; Husain, M. M.; Heiskanen, K. M.; Mukhtar, H. Differential antiproliferative and apoptotic response of sanguinarine for cancer cells versus normal cells. *Clin. Cancer Res.* **2000**, *6* (4), 1524-1528.
- [67] Wolff, J.; Knipling, L. Antimicrotubule properties of benzo-phenanthridine alkaloids. *Biochemistry* **1993**, *32* (48), 13334-13339.
- [68] Slaninova, I.; Taborska, E.; Bochorakova, H.; Slanina, J. Interaction of benzo[c]phenanthridine and protoberberine alkaloids with animal and yeast cells. *Cell Biol. Toxicol.* **2001**, *17* (1), 51-63.
- [69] Beuria, T. K.; Santra, M. K.; Panda, D. Sanguinarine Blocks Cytokinesis in Bacteria by Inhibiting FtsZ Assembly and Bundling. *Biochemistry* **2005**, *44* (50), 16584-16593.
- [70] White, E. L.; Ross, L. J.; Reynolds, R. C.; Seitz, L. E.; Moore, G. D.; Borhani, D. W. Slow polymerization of Mycobacterium tuberculosis FtsZ. *J. Bacteriol.* **2000**, *182* (14), 4028-4034.
- [71] Mazumdar, M.; Parrack, P. K.; Mukhopadhyay, K.; Bhattacharyya, B. Bis-ANS as a specific inhibitor for microtubule-associated protein-induced assembly of tubulin. *Biochemistry* **1992**, *31* (28), 6470-6474.
- [72] Yu, X. C.; Margolin, W. Inhibition of assembly of bacterial cell division protein FtsZ by the hydrophobic dye 5,5'-bis-(8-anilino-1-naphthalenesulfonate). *J. Biol. Chem.* **1998**, *273* (17), 10216-22.
- [73] Nair, P. Biochemical Assays and Inhibitor Studies. *PHD Thesis* **2004**, (Chapter Two).
- [74] Slayden, R. A.; Tonge, P. J. Unpublished results.
- [75] Sarcina, M.; Mullineaux, C. W. Effects of tubulin assembly inhibitors on cell division in prokaryotes *in vivo*. *FEMS Microbiol. Lett.* **2000**, *191* (1), 25-9.
- [76] Slayden, R. A.; Knudson, D. L.; Belisle, J. T. Morphological and Transcriptional Characterization of the Inhibition of Septum Formation in Mycobacterium tuberculosis. *Microbiology* **2006** *in press*.
- [77] White, E. L.; Suling, W. J.; Ross, L. J.; Seitz, L. E.; Reynolds, R. C. 2-Alkoxy-carbonylaminopyridines: inhibitors of Mycobacterium tuberculosis FtsZ. *J. Antimicrob. Chemother.* **2002**, *50* (1), 111-114.
- [78] Reynolds, R. C.; Srivastava, S.; Ross, L. J.; Suling, W. J.; White, E. L. A new 2-carbamoyl pteridine that inhibits mycobacterial FtsZ. *Bioorg. Med. Chem. Lett.* **2004**, *14* (12), 3161-3164.
- [79] White, L. E.; Reynolds, R. C.; Suling, W. Antimicrobial inhibitors of FtsZ protein. WO2004005472, 2004.
- [80] Huang, Q.; Kirikae, F.; Kirikae, T.; Pepe, A.; Amin, A.; Respicio, L.; Slayden, R. A.; Tonge, P. J.; Ojima, I. Targeting FtsZ for Antituberculosis Drug Discovery: Noncytotoxic Taxanes as Novel Antituberculosis Agents. *J. Med. Chem.* **2006**, *49* (2), 463-466.
- [81] Huang, Q.; Pepe, A.; Zanardi, I.; Tonge, P. J.; Slayden, R. A.; Kirikae, F.; Kirikae, T.; Ojima, I. Targeting FtsZ for anti-tuberculosis drug discovery: non-cytotoxic taxanes as novel anti-TB agents. *Abstracts of Papers, 229th ACS National Meeting, San Diego, CA, United States, 2005*, MEDI-386.
- [82] Georg, G. I.; Chen, T. T.; Ojima, I.; Wyas, D. M.; Eds. Taxane Anticancer Agents: Basic Science and Current Status. *ACS Symp. Ser.* **1995**, *583*, 1-353.
- [83] Ojima, I.; Kuduk, S. D.; Chakravarty, S. Recent advances in the medicinal chemistry of taxoid anticancer agents. *Adv. Med. Chem.* **1999**, *4*, 69-124.
- [84] Kingston, D. G. I.; Jagtap, P. G.; Yuan, H.; Samala, L. The chemistry of taxol and related taxoids. *Progress in the chemistry of organic natural products* **2002**, *84*, 53-225.
- [85] Ojima, I.; Bounaud, P.-Y.; Takeuchi, C.; Pera, P.; Bernacki, R. J. New taxanes as highly efficient reversal agents for multi-drug resistance in cancer cells. *Bioorg. Med. Chem. Lett.* **1998**, *8* (2), 189-194.
- [86] Ojima, I.; Bounaud, P.-Y.; Bernacki, R. J. New weapons in the fight against cancer. *Chemtech* **1998**, *28* (6), 31-36.
- [87] Ojima, I.; Bounaud, P.-Y.; Oderda, C. F. Recent strategies for the treatment of multi-drug resistance in cancer cells. *Expert Opin. Ther. Pat.* **1998**, *8* (12), 1587-1598.
- [88] Ojima, I.; Bounaud, P.-Y.; Bernacki, R. J. Designing taxanes to treat multidrug-resistant tumors. *Mod. Drug Disc.* **1999**, *2* (3), 45,47-48,51-52.
- [89] Brooks, T.; Minderman, H.; O'Loughlin, K. L.; Pera, P.; Ojima, I.; Baer, M. R.; Bernacki, R. J. Taxane-based reversal agents modulate drug resistance mediated by P-glycoprotein, multidrug resistance protein, and breast cancer resistance protein. *Mol. Cancer Ther.* **2003**, *2* (11), 1195-1205.
- [90] Minderman, H.; Brooks, T. A.; O'Loughlin, K. L.; Ojima, I.; Bernacki, R. J.; Baer, M. R. Broad-spectrum modulation of ATP-binding cassette transport proteins by the taxane derivatives ortataxel (IDN-5109, BAY 59-8862) and tRA96023. *Cancer Chemoth. Pharm.* **2004**, *53* (5), 363-369.

- [91] Brooks, T. A.; Kennedy, D. R.; Gruol, D. J.; Ojima, I.; Baer, M. R.; Bernacki, R. J. Structure-activity analysis of taxane-based broad-spectrum multidrug resistance modulators. *Anticancer Res.* **2004**, *24* (2A), 409-415.
- [92] Ojima, I.; Borella, C. P.; Wu, X.; Bounaud, P.-Y.; Oderda, C. F.; Sturm, M.; Miller, M. L.; Chakravarty, S.; Chen, J.; Huang, Q.; Pera, P.; Brooks, T. A.; Baer, M. R.; Bernacki, R. J. Design, Synthesis and Structure-Activity Relationships of Novel Taxane-Based Multidrug Resistance Reversal Agents. *J. Med. Chem.* **2005**, *48* (6), 2218-2228.
- [93] Georg, G. I.; Harriman, G. C. B.; Vander Velde, D. G.; Boge, T. C.; Cheruvallath, Z. S.; Datta, A.; Hepperle, M.; Park, H.; Himes, R. H.; Jayasinghe, L. Medicinal chemistry of paclitaxel. Chemistry, structure-activity relationships, and conformational analysis. *ACS Symp. Ser.* **1995**, *583* (Taxane Anticancer Agents), 217-232.
- [94] Appendino, G.; Danieli, B.; Jakupovic, J.; Belloro, E.; Scambia, G.; Bombardelli, E. The chemistry and occurrence of taxane derivatives. XXX. Synthesis and evaluation of C-seco paclitaxel analogs. *Tetrahedron Lett.* **1997**, *38* (24), 4273-4276.
- [95] Taraboletti, G.; Micheletti, G.; Rieppi, M.; Poli, M.; Turatto, M.; Rossi, C.; Borsotti, P.; Roccabianca, P.; Scanziani, E.; Nicoletti, M. I.; Bombardelli, E.; Morazzoni, P.; Riva, A.; Giavazzi, R. Antiangiogenic and antitumor activity of IDN 5390, a new taxane derivative. *Clin. Cancer Res.* **2002**, *8* (4), 1182-1188.

Received: February 18, 2006

Accepted: March 15, 2006

Development and Evaluation of a Line Probe Assay for Rapid Identification of *pncA* Mutations in Pyrazinamide-Resistant *Mycobacterium tuberculosis* Strains[∇]

Jun-Ichiro Sekiguchi,¹ Tomohiko Nakamura,² Tohru Miyoshi-Akiyama,¹ Fumiko Kirikae,¹ Intetsu Kobayashi,³ Ewa Augustynowicz-Kopeć,⁴ Zofia Zwolska,⁴ Koji Morita,⁵ Toshinori Suetake,² Hiroshi Yoshida,² Seiya Kato,⁶ Toru Mori,⁷ and Teruo Kirikae^{1*}

Department of Infectious Diseases, Research Institute, International Medical Center of Japan, 1-21-1 Toyama, Shinjuku, Tokyo 162-8655, Japan¹; Third Department, Research and Development Laboratory, Nipro Corporation, 3023 Noji, Kusatsu, Shiga 525-0055, Japan²; Mitsubishi Chemical Medience Corporation, 3-30-1 Shimura, Itabashi, Tokyo 174-8555, Japan³; National Research Institute of Tuberculosis and Lung Diseases, Plocka St. 26, Warsaw 01-138, Poland⁴; Department of Microbiology, Kyorin University School of Health Sciences, 476 Miyashita, Hachioji, Tokyo 192-8508, Japan⁵; Research Institute of Tuberculosis, Japan Anti-Tuberculosis Association, Matsuyama 3-1-24, Kiyose, Tokyo 204-8533, Japan⁶; and Leprosy Research Center, National Institute of Infectious Diseases, Aoba 4-2-1, Higashimurayama, Tokyo 189-0002, Japan⁷

Received 14 February 2007/Returned for modification 28 March 2007/Accepted 19 June 2007

Resistance of *Mycobacterium tuberculosis* to pyrazinamide (PZA) derives mainly from mutations in the *pncA* gene. We developed a reverse hybridization-based line probe assay with oligonucleotide probes designed to detect mutations in *pncA*. The detection of PZA resistance was evaluated in 258 clinical isolates of *M. tuberculosis*. The sensitivity and specificity of PZA resistance obtained by this new assay were both 100%, consistent with the results of conventional PZA susceptibility testing. This assay can be used with sputa from tuberculosis patients. It appears to be reliable and widely applicable and, given its simplicity and rapid performance, will be a valuable tool for diagnostic use.

Pyrazinamide (PZA) is an important first-line antituberculosis drug used clinically for short-course chemotherapy because of its effectiveness against semidormant bacilli sequestered within macrophages (6, 10). The intracellular sterilizing activity of PZA allows the treatment period to be reduced to 6 months, whereas 9 months of treatment is required when PZA is not used (19). PZA is a prodrug. It requires conversion to pyrazinoic acid by bacterial pyrazinamidase (PZase) to affect tuberculosis bacilli (7, 17). Recent reports have established that mutations in the PZase gene (*pncA*) lead to the loss of PZase activity and constitute the primary mechanism of PZA resistance in *Mycobacterium tuberculosis* (11, 21, 22).

The time required for in vitro drug susceptibility testing of *M. tuberculosis* is constrained by the organism's relatively slow growth. Conventional drug susceptibility testing takes 7 to 28 days, depending on the culture system used (15). For most antituberculosis drugs, conventional methods produce reliable results, although PZA susceptibility testing with such methods is impaired by the poor bacterial growth under acidic conditions (7, 9). However, new culture methods were developed recently to resolve this problem (2, 13).

Previously, we described a DNA sequencing-based method to detect mutations in the genome of drug-resistant strains, including PZA-resistant *M. tuberculosis* (18). However, the use

of this method in ordinary-scale clinical laboratories can be difficult. Therefore, we developed and describe here a new hybridization-based line probe assay (LiPA) for the rapid detection of *pncA* mutations in *M. tuberculosis* that is easily applied to clinical use. This assay can be used to evaluate PZA resistance, particularly in multidrug-resistant organisms, analyze PZA-resistant genes, and identify epidemic strains.

MATERIALS AND METHODS

Bacterial strains. Two hundred twenty-five clinical isolates of *M. tuberculosis* were obtained from patients with pulmonary tuberculosis in Japan, and 33 were obtained from patients in Poland. The other bacterial strains used in this study are listed in Table 1.

Clinical samples. Fifty-three sputum samples were collected from patients with tuberculosis or suspected tuberculosis. These samples were treated with an *N*-acetyl-L-cysteine-NaOH solution according to the procedure provided with the BBL MycoPrep Mycobacterial System Digestion/Decontamination kit (BD Diagnostic Systems, Franklin Lakes, NJ). Each sample was suspended in 1.5 ml of phosphate buffer. One milliliter of the suspension was transferred into a 1.5-ml tube. The remaining suspension was inoculated onto Ogawa medium and into MGIT 960 broth (BD BACTEC MGIT 960; BD Biosciences) and cultured for mycobacterial examination. One milliliter of the suspension was centrifuged for 15 min at 13,000 × *g*, and the supernatant was removed with a pipette. Tris-EDTA (TE) buffer (100 μl) was added to the sediment, and the solution was again centrifuged for 15 min at 13,000 × *g*. The sediment was suspended in 50 μl of TE buffer (50 μl), resuspended by vortexing, and incubated at 95°C for 30 min followed by incubation at 100°C for 10 min. The sample was vortexed again, allowed to cool, and centrifuged at 12,000 × *g* for 5 min to clarify the supernatant, which was transferred into another 1.5-ml tube. Each aliquot of the supernatant (5 μl) was used for each of the LiPA or Cobas Amplicor assays (Roche Diagnostic Systems, Basel, Switzerland).

PZA susceptibility testing and assay for PZase activity. All clinical isolates of *M. tuberculosis* and *M. tuberculosis* strains H37Rv and H37Ra were tested for PZA susceptibility. Susceptibility to PZA was assessed by the broth method

* Corresponding author. Mailing address: Department of Infectious Diseases, Research Institute, International Medical Center of Japan, 1-21-1 Toyama, Shinjuku, Tokyo 162-8655, Japan. Phone: (81) 3 3202 7181, ext. 2838. Fax: (81) 3 3202 7364. E-mail: tkirikae@ri.imcj.go.jp.

[∇] Published ahead of print on 27 June 2007.

TABLE 1. Species specificity of the LiPA for detecting *M. tuberculosis pncA*

Species	Strain ^a	Nested PCR result ^b	Hybridization signal with probes:	
			1-24	25-47
<i>M. tuberculosis</i>	H37Rv (ATCC 27294)	+	All positive	All positive
<i>M. tuberculosis</i>	H37Ra (ATCC 25177)	+	All positive	All positive
<i>M. bovis</i>	BCG Japanese strain 172 ^c	+	Δ16 ^d	All positive
<i>M. avium</i>	ATCC 25291	-*	All negative	All negative
<i>M. fortuitum</i>	RIMD 1317004 (ATCC 6841)	-*	All negative	All negative
<i>M. gastri</i>	GTC 610 (ATCC 15754)	-*	All negative	All negative
<i>M. intracellulare</i>	JCM 6384 (ATCC 13950)	-*	All negative	All negative
<i>M. kansasii</i>	JCM 6379 (ATCC 124878)	-	All negative	All negative
<i>M. marinum</i>	GTC 616 (ATCC 927)	-*	All negative	All negative
<i>M. nonchromogenicum</i>	JCM 6364 (ATCC 19530)	-*	All negative	All negative
<i>M. phlei</i>	RIMD 1326001 (ATCC 19249)	-	All negative	All negative
<i>M. scrofulaceum</i>	JCM 6381 (ATCC 19981)	-	All negative	All negative
<i>M. simiae</i>	GTC 620 (ATCC 25275)	-	All negative	All negative
<i>M. smegmatis</i>	ATCC 19420	-	All negative	All negative
<i>M. szulgai</i>	JCM 6383 (ATCC 35799)	-	All negative	All negative
<i>M. terrae</i>	GTC 623 (ATCC 15755)	-	All negative	All negative
<i>Escherichia coli</i>	ATCC 8739	-	All negative	All negative
<i>Haemophilus influenzae</i>	IID 984 (ATCC 9334)	-	All negative	All negative
<i>Klebsiella pneumoniae</i>	IID5209 (ATCC 15380)	-	All negative	All negative
<i>Legionella pneumophila</i>	GTC 745	-	All negative	All negative
<i>Mycoplasma pneumoniae</i>	IID 817	-	All negative	All negative
<i>Pseudomonas aeruginosa</i>	ATCC 27853	-	All negative	All negative
<i>Rhodococcus equi</i>	ATCC 33710	-	All negative	All negative
<i>Staphylococcus aureus</i>	N315	-	All negative	All negative
<i>Streptococcus pneumoniae</i>	GTC 261	-	All negative	All negative

^a ATCC, American Type Culture Collection, Manassas, VA; RIMD, Research Institute for Microbial Diseases, Osaka University, Osaka, Japan; GTC, Gifu Type Culture Collection, Department of Microbiology-Bioinformatics, Regeneration and Advanced Medical Science, Gifu University, Graduate School of Medicine, Bacterial Genetic Resources, Gifu, Japan; JCM, Japan Collection of Microorganisms, Institute of Physical and Chemical Research (RIKEN), Saitama, Japan; IID, Institute of Medical Science, University of Tokyo, Tokyo, Japan.

^b Approximately 100 ng of genomic DNA was used in the first PCR. Amplification results were determined by agarose gel electrophoresis. +, presence of amplification product of the expected; -, absence of amplification products; -*, presence of amplification products, but the sizes of the products were different from that of *M. tuberculosis*.

^c From Japan BCG Laboratory, Tokyo, Japan.

^d Absence of hybridization signal with one of the probes (probe 16).

(MGIT 960). Nontuberculous *Mycobacterium* spp. were also tested for PZA susceptibility with the MGIT 960 method. However, standard methods for susceptibility testing are not available for nontuberculous *Mycobacterium* spp. (5). PZase activity was determined as described previously (20). In brief, a heavy loopful of mycobacterial culture freshly grown on Ogawa medium was inoculated onto 5 ml of Middlebrook 7H11 agar supplemented with pyrazinocarboxamide (0.812 mM; Wako Pure Chemical Industries, Osaka, Japan), sodium pyruvate (18.18 mM; Nacalai Tesque, Kyoto, Japan), and glycerol (0.5%, vol/vol; Nacalai) in a glass tube with a screw cap. After incubation at 37°C for 4 days, 1 ml of freshly prepared ferrous ammonium sulfate solution (25.5 mM; Sigma Chemical, St. Louis, MO) was added to each tube, and the presence of a pink band was assessed. *M. tuberculosis* strain H37Rv, which is susceptible to PZA and positive for PZase, was used as a positive control for the assay. *M. bovis* strain BCG, which is resistant to PZA and negative for PZase, was used as a negative control.

DNA extraction. Two different methods were applied to extract genomic DNA. One method was described previously (12). The other method was performed as follows. Mycobacterial cells and other bacterial cells were collected from Ogawa medium and broth medium, respectively. A loopful of cells was suspended in 0.5 ml 1× TE buffer and inactivated at 100°C for 10 min. Cellular debris was pelleted at 13,000 × g for 5 min, and the supernatant with genomic DNA was used for PCR. Mycobacterial DNA in sputa was extracted with a cell lysis solution contained in a diagnosis kit (Amplicor respiratory specimen preparation kit; Roche Molecular Systems, Inc., Branchburg, NJ) or extracted by heating at 95°C for 30 min followed by freezing and thawing.

Preparation of oligonucleotide probes and strips. Forty-seven oligonucleotide probes were designed to cover the entire *pncA* gene of wild-type H37Rv (Fig. 1). Two oligonucleotide probes were designed to compensate for silent mutations of C to T at nucleotide positions 180 and 195. A total of 49 probes were synthesized. These probes were immobilized on two strips. One strip contained 24 probes (probes 1 to 24) plus two probes to compensate for silent mutations. The other contained 23 probes (probes 25 to 47).

LiPA. The LiPA described here was developed on the basis of the same principle as that of the commercially available INNO-LiPA Rif. TB kit (Innogenetics, Ghent, Belgium) for the detection of rifampin resistance (14). The LiPA was conducted as described previously (14). In brief, biotinylated PCR products from test samples were hybridized to the immobilized probes and washed under strict conditions (1× SSC [1× SSC is 0.15 M NaCl plus 0.015 M sodium citrate] buffer containing 0.1% sodium dodecyl sulfate at 62°C). The presence or absence of bands on all strips was judged independently by three different observers. The classifications by the three observers were identical. Genomic DNA from the PZA-susceptible H37Rv strain was used as a positive control. Results for all samples were compared to those for the positive control. DNA from *M. tuberculosis* H37Rv was diluted into TE buffer (final concentrations, 4.84 pg/μl, 484 fg/μl, 242 fg/μl, 48.4 fg/μl, 24.2 fg/μl, and 2.42 fg/μl), and 1 μl of each solution was used to determine the sensitivity of the LiPA.

PCR and DNA sequencing. Unless otherwise indicated, approximately 2 to 5 ng of genomic DNA was used for the amplification of a 670-bp fragment that includes the complete open reading frame of the *pncA* gene. To increase the sensitivity, nested PCR was performed with unlabeled external primers PR9-1 (5'-GGC GTC ATG GAC CCT ATA TCT G-3') and PR10-1 (5'-CTT GCG GCG AGC GCT C-3') for the first PCR and biotin-labeled internal primers IP-F (5'-GCT GCG GTA GGC AAA CTG C-3') and IP-R (5'-CCA ACA GTT CAT CCC GGT TCG-3') for the second PCR. The amplification conditions for the first and second PCRs were the same and consisted of 5 min of denaturation at 95°C followed by 40 cycles of 1 min at 95°C, 1 min at 55°C, and 1 min at 72°C. In some experiments, only the second PCR was done. Sequencing of *pncA* and its promoter region (nucleotides -80 to 572 relative to the initiation codon) was performed as described previously (18) for *M. tuberculosis* H37Rv and H37Ra, *Mycobacterium bovis* BCG, and all 258 clinical *M. tuberculosis* isolates tested regardless of the LiPA results.

COBAS Amplicor assays. COBAS Amplicor assays, including the Amplicor MTB test, Amplicor *M. avium* test, and Amplicor *M. intracellulare* test (Roche

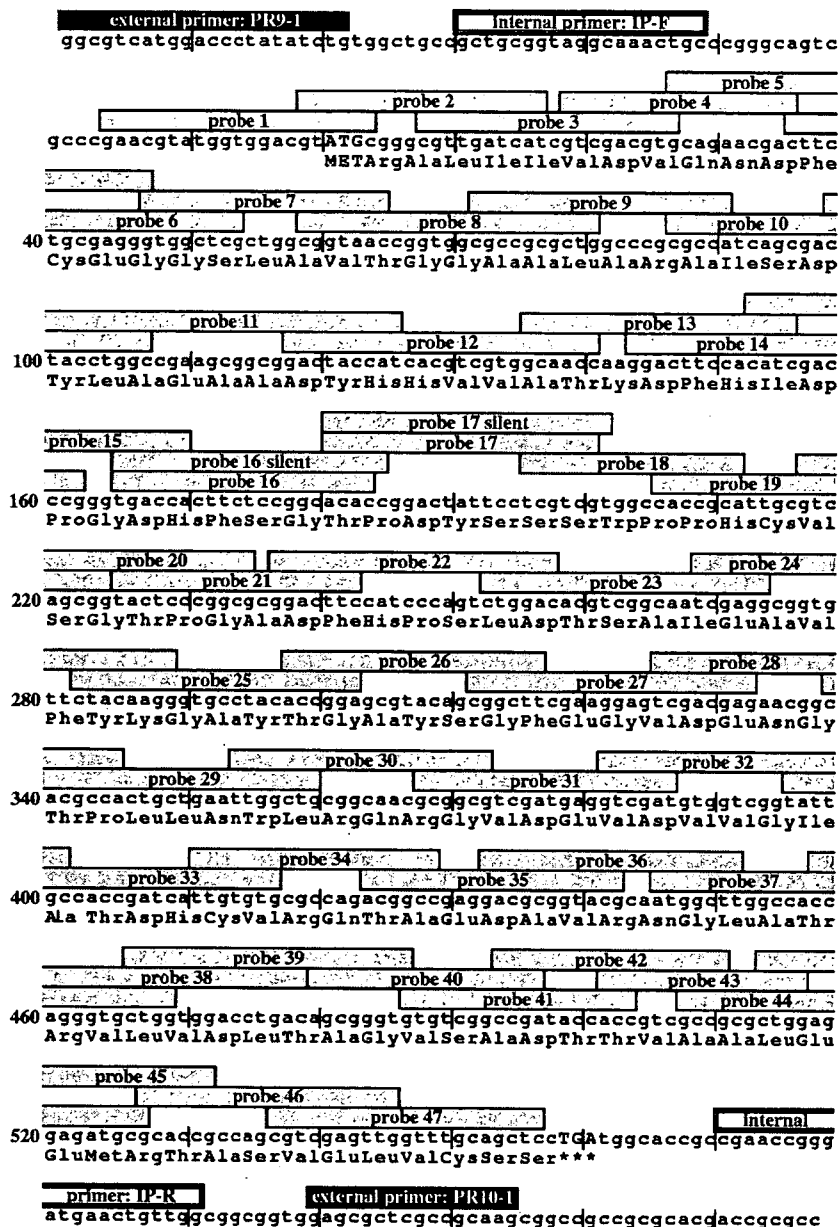


FIG. 1. Locations of 49 oligonucleotide probes designed to cover the *pncA* gene of *M. tuberculosis* H37Rv.

Diagnostic Systems), were performed according to the instructions provided by the manufacturer.

RESULTS AND DISCUSSION

Among the 25 bacterial strains listed in Table 1, three strains, *M. tuberculosis* H37Rv, *M. tuberculosis* H37Ra, and *M. bovis* BCG, yielded PCR products of the expected length (approximately 600 bp). The other 13 strains of nontuberculous *Mycobacterium* spp. and nine strains of nonmycobacterial spp. yielded products of different lengths or were not amplified to a level detectable in agarose gels (Table 1). In the LiPA, PCR products from *M. tuberculosis* strains hybridized with all of the *pncA* probes (Table 1). LiPA results for strain H37Rv are shown in Fig. 2 (lane 1). The *M. bovis* product hybridized with

all probes except for probe 16 (Table 1 and Fig. 2, lane 22). All other bacteria tested showed no hybridization with any of the probes (data not shown). These data indicate that the LiPA is specific for *M. tuberculosis* and *M. bovis*.

Sensitivity of the LiPA with the nested PCR was 24.2 fg of *M. tuberculosis* DNA, which is equivalent to five copies of the *pncA* gene (data not shown), whereas when only the second PCR was done, the sensitivity of the LiPA was 484 fg, which is equivalent to 1,000 copies of *pncA* (data not shown). These data suggest that nested PCR is needed to yield the higher sensitivity.

Of 258 clinical isolates of *M. tuberculosis* tested with the LiPA, 228 were wild type, and the other 30 showed at least one mutation pattern (Table 2). Representative LiPA patterns are

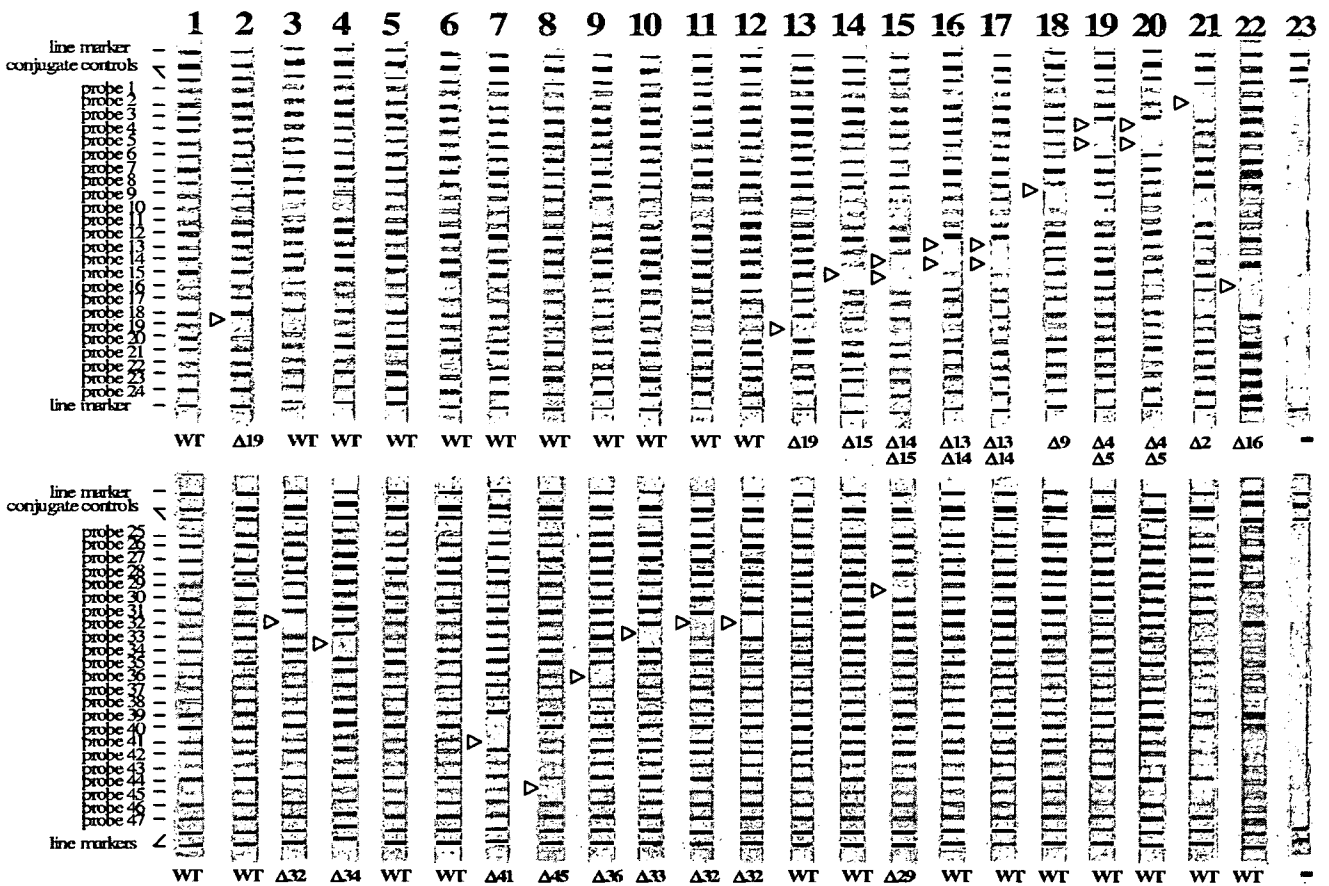


FIG. 2. Representative patterns of isolates that had a mutation(s) according to the LiPA for detection of *pncA* mutations. Positions of the oligonucleotides, conjugate control lines, and marker lines are shown. A negative signal is shown by an open triangle. LiPA patterns of *M. tuberculosis* strains are shown in lanes 1 to 21. Lanes: 1, H37Rv; 2, IMCJ(130); 3, IMCJ904III; 4, IMCJ(66); 5, IMCJ(85); 6, IMCJ(67); 7, 13229; 8, IMCJ.M22; 9, P26; 10, 13243; 11, IMCJ850; 12, IMCJ835; 13, IMCJ501; 14, IMCJ844; 15, IMCJ479; 16, IMCJ843; 17, P12; 18, IMCJ901III; 19, IMCJ(80); 20, P10; 21, IMCJ.K1; 22, *M. bovis* BCG Japanese strain 172; 23, no DNA. WT, wild-type *pncA*.

shown in Fig. 2. Hybridization signals visualized as violet bands on the strips were strong and readily discernible, with low background, although there was variability in bands intensities, and some strains yielded less intense bands than others. The 228 isolates hybridized to all probes, as shown by the data for strain H37Rv in Fig. 2 (lane 1). The products of the other 30 *M. tuberculosis* strains containing a mutation(s) did not hybridize to the probes corresponding to the position of the mutation(s) but did hybridize to the others. These results were fully consistent with the DNA sequencing results (Table 2). DNA sequencing confirmed that *pncA* of BCG had a C-to-G point mutation at codon 59, causing histidine to become aspartic acid (Table 2). These data are consistent with our previous findings and those of others (17, 18) showing that *M. bovis* BCG is naturally resistant to PZA. In addition, of the 13 other non-tuberculous *Mycobacterium* spp. listed in Table 1, *M. gastri* was susceptible to PZA. All others were resistant to PZA (data not shown).

Regarding the PZA resistance profile, the LiPA yielded results that were 100% in agreement with those obtained by the culture-based susceptibility method (Table 3). In addition, all PZase-positive bacilli were sensitive to PZA, and all PZase-negative bacilli were resistant to PZA (Table 2). These data

were consistent with those of previously published reports (18, 22). The LiPA correctly identified PZA susceptibility and resistance in all strains in which a mutation(s) occurred. All of the 30 PZA-resistant *M. tuberculosis* isolates were correctly identified as being PZA resistant by the LiPA, and all of the 228 PZA-susceptible isolates were identified as being PZA susceptible. The specificity, sensitivity, and positive and negative predictive values of the LiPA for the detection of PZA resistance were all 100% (Table 3). In addition, we determined PZase activities of all *Mycobacterium* spp. listed in Table 1 and all clinical isolates of *M. tuberculosis* tested. Strains with PZase activity were sensitive to PZA, and those without PZase activity were resistant to PZA (data not shown).

To examine whether the LiPA can be applied to clinical samples from patients with tuberculosis, sputum samples obtained from 53 patients with suspected tuberculosis were tested (data not shown). All samples were positive for acid-fast staining. Among these 53 samples, 46 were positive for tuberculosis by the Amplicor MTB test and/or mycobacterial culture, and six were positive for *M. avium* by the Amplicor *M. avium* test. The remaining sample was positive for acid-fast staining but PCR and culture negative. In 45 of the 46 samples, *M. tuberculosis pncA* was detected with the LiPA. However, no muta-

TABLE 2. Identification of *pncA* mutations by LiPA among 258 clinical isolates of *M. tuberculosis* and *M. bovis* BCG

Strain	LiPA profile ^a	Mutation		PZA susceptibility	PZase activity
		Amino acid change	Variant nucleotides		
IMCJ.K1	Δ2	3 Ala→Glu	GCG→GAG	R	-
P10	Δ4, Δ5	10 Gln→Pro	CAG→CCG	R	-
IMCJ(80)	Δ4, Δ5	12 Asp→Ala	GAC→GCC	R	-
IMCJ693	Δ4, Δ5	12 Asp→Ala	GAC→GCC	R	-
IMCJ(120)	Δ4, Δ5	12 Asp→Ala	GAC→GCC	R	-
IMCJ901III	Δ8, Δ9	27 Leu→Pro	CTG→CGC	R	-
IMCJ918III	Δ8, Δ9	27 Leu→Pro	CTG→CGC	R	-
P12	Δ13, Δ14	51 His→Gln	CAC→CAG	R	-
IMCJ843	Δ13, Δ14	51 His→Gln	CAC→CAA	R	-
IMCJ846	Δ13, Δ14	51 His→Gln	CAC→CAA	R	-
IMCJ479	Δ14, Δ15, Δ29	53 Asp→Asn frameshift	GAC→AAC, 349 insertion CACTG	R	-
IMCJ844	Δ15	54 Pro→Leu	CCG→CTG	R	-
IMCJ695	Δ15	54 Pro→Leu	CCG→CTG	R	-
IMCJ838	Δ15	54 Pro→Leu	CCG→CTG	R	-
IMCJ29	Δ15	54 Pro→Leu	CCG→CTG	R	-
IMCJ907III	Δ15	54 Pro→Leu	CCG→CTG	R	-
IMCJ908III	Δ15	54 Pro→Leu	CCG→CTG	R	-
IMCJ501	Δ19	72 Cys→Trp	TGC→TGG	R	-
IMCJ(133)	Δ19	72 Cys→Trp	TGC→TGG	R	-
IMCJ(130)	Δ19	Frameshift	218 insertion CGCATT GCCG	R	-
IMCJ835	Δ32	132 Gly→Ser	GGT→AGT	R	-
IMCJ849	Δ32	132 Gly→Ser	GGT→AGT	R	-
IMCJ850	Δ32	133 Ile→Thr	ATT→ACT	R	-
IMCJ837	Δ32	133 Ile→Thr	ATT→ACT	R	-
IMCJ904III	Δ32	Frameshift	386-388 deletion ATG	R	-
13243	Δ33	136 Asp→Tyr	GAT→TAT	R	ND
IMCJ(66)	Δ34	Frameshift	420 insertion G	R	-
P26	Δ36	148 Arg→Ser	CGC→AGC	R	-
13229	Δ41	Frameshift	493 insertion C	R	ND
IMCJ.M22	Δ45	175 Met→Val	ATG→GTG	R	-
IMCJ(67)	Wild type (Δ16) ^b	(60 Gly→Gly)	(GGC→GGT silent)	S	+
IMCJ(134)	Wild type (Δ16)	(60 Gly→Gly)	(GGC→GGT silent)	S	+
IMCJ(85)	Wild type (Δ17)	(65 Ser→Ser)	(TCC→TCT silent)	S	+
IMCJ(75)	Wild type (Δ17)	(65 Ser→Ser)	(TCC→TCT silent)	S	+
IMCJ851	Wild type (Δ17)	(65 Ser→Ser)	(TCC→TCT silent)	S	+
IMCJ839	Wild type (Δ17)	(65 Ser→Ser)	(TCC→TCT silent)	S	+
IMCJ(90)	Wild type (Δ17)	(65 Ser→Ser)	(TCC→TCT silent)	S	+
IMCJ(96)	Wild type (Δ17)	(65 Ser→Ser)	(TCC→TCT silent)	S	+
IMCJ(125)	Wild type (Δ17)	(65 Ser→Ser)	(TCC→TCT silent)	S	+
H37Rv	Wild type	No change	No change	S	+
BCG ^c	Δ16	59 His→Asp	CAC→GAC	R	-

^a Δ indicates the negative signal at any of the probes.

^b Δ in parentheses indicates the negative signal at any of the probes unless the probe to compensate for the silent mutation was used.

^c *M. bovis* BCG Japanese strain 172.

tion of *pncA* was found in these 45 samples, suggesting that all of the samples contained PZA-sensitive organisms. These results were later confirmed by drug susceptibility testing when *M. tuberculosis* isolates were obtained from the samples. Hybridization was not detected on the strips in the six *M. avium*-positive samples as well as the remaining sample that was

positive for acid-fast staining but negative for PCR and culture. All samples were culture positive for mycobacteria. These results indicate that the LiPA is applicable to clinical samples. However, further studies of clinical samples containing PZA-resistant *M. tuberculosis* are necessary.

It appears that nested PCR rarely introduces additional mu-

TABLE 3. Diagnostic performance of the LiPA compared to PZA susceptibility testing

Result by PZA susceptibility test	No. of <i>M. tuberculosis</i> clinical isolates (n = 258)	LiPA result		Sensitivity (%)	Specificity (%)	Predictive value (%)	
		No. resistant	No. susceptible			Positive	Negative
Resistant	30	30	0	100	100	100	100
Susceptible	228	0	228 ^a				

^a Includes nine isolates with a silent mutation in *pncA*.

tations that may lead to false-positive results for the LiPA. *Taq* DNA polymerase is reported to make one error every 120 bases, and it was reported that these errors occur randomly (3). To affect LiPA results, the error must occur very early in the amplification process and at a specific site causing false-positive results in almost all PCR products. The frequency may be $3 \times 10^{-11} [(1/120)^5]$ when there are five copies of the template. In fact, nested PCR is used for other LiPA assays (1, 8) and for single-strand conformation polymorphism analysis (4).

We showed the usefulness of the LiPA for PZA susceptibility testing of *M. tuberculosis*. This assay can detect *M. tuberculosis* in smear-positive sputa from patients. This LiPA can rapidly and efficiently assess the resistance of *M. tuberculosis* to PZA. It is simple, convenient, and highly reliable when run in parallel with a convenient *M. tuberculosis* diagnostic algorithm in laboratories. However, the LiPA has some limitations. First, this assay does not have an internal control. In addition, this assay cannot correctly identify mixed PZA-resistant and -susceptible isolates. This assay cannot detect novel silent mutations; however, it can detect known mutations. Finally, genes other than *pncA* may be associated with PZA resistance. Scorpio et al. (16) previously reported PZase-positive PZA-resistant *M. tuberculosis* strains that were very rare and usually showed a low level of resistance. Nevertheless, our LiPA is a valuable tool for the detection of resistant *M. tuberculosis* strains within one working day and can easily be included in the routine workflow.

ACKNOWLEDGMENTS

We thank M. Nakano (Jichi Medical School, Tochigi, Japan) for comments on the manuscript.

This study was supported by Health Sciences Research grants from the Ministry of Health, Labor, and Welfare of Japan (H15-SHINKO-3 and H18-SHINKO-IPPAN-012) and by the Program of Founding Research Centers for Emerging and Reemerging Infectious Diseases of the Ministry of Education, Culture, Sports, Science and Technology of Japan.

REFERENCES

1. Beenhouwer, H. D., Z. Lhiang, G. Jannes, W. Mijs, L. Machtelinckx, R. Rossau, H. Traore, and F. Portaels. 1995. Rapid detection of rifampicin resistance in sputum and biopsy specimens from tuberculosis patients by PCR and line probe assay. *Tuber. Lung Dis.* 76:425-430.
2. Bemer, P., T. Bodmer, J. Munzinger, M. Perrin, V. Vicent, and H. Drugeon. 2004. Multicenter evaluation of the MB/BACT system for susceptibility testing of *Mycobacterium tuberculosis*. *J. Clin. Microbiol.* 42:1030-1034.
3. Benjamin, B. D., and B. A. Connolly. 2004. Low-fidelity *Pyrococcus furiosus* DNA polymerase mutants useful in error-prone PCR. *Nucleic Acids Res.* 32:e176.
4. Bum-joon, K., K. H. Lee, B. N. Park, S. J. Kim, E. M. Park, Y. G. Park, G. H. Bai, S. J. Kim, and Y. H. Kook. 2001. Detection of rifampin-resistant *Mycobacterium tuberculosis* in sputa by nested PCR-linked single-strand conformation polymorphism and DNA sequencing. *J. Clin. Microbiol.* 39:2610-2617.
5. Clinical and Laboratory Standards Institute. 2000. Susceptibility testing of mycobacteria, nocardia, and other aerobic actinomycetes. Approved standard M24-A. Clinical and Laboratory Standards Institute, Wayne, PA.
6. Heifets, L., and P. Lindholm-Levy. 1992. Pyrazinamide sterilizing activity *in vitro* against semidormant *Mycobacterium tuberculosis* bacterial populations. *Am. Rev. Respir. Dis.* 145:1223-1225.
7. Konno, K., F. M. Feldmann, and W. McDermott. 1967. Pyrazinamide susceptibility and amidase activity of tubercle bacilli. *Am. Rev. Respir. Dis.* 95:461-469.
8. Marttila, H. J., H. Soini, E. Vyshnevskaya, B. I. Vishnevskiy, T. F. Otten, A. V. Vasilyef, and M. K. Viljamen. 1999. Line probe assay in the rapid detection of rifampin-resistant *Mycobacterium tuberculosis* directly from clinical specimens. *Scand. J. Infect. Dis.* 31:269-273.
9. McDermott, W., and R. Tompsett. 1954. Activation of pyrazinamide and nicotinamide in acidic environments *in vitro*. *Am. Rev. Tuberc.* 70:748-754.
10. Mitchison, D. A. 1985. The action of antituberculosis drugs in short-course chemotherapy. *Tubercle* 66:219-225.
11. Morlock, G. P., J. T. Crawford, W. R. Butler, S. E. Brim, D. Sikes, G. H. Mazurek, C. L. Woodley, and R. C. Cooksey. 2000. Phenotypic characterization of *pncA* mutants of *Mycobacterium tuberculosis*. *Antimicrob. Agents Chemother.* 44:2291-2295.
12. Otsuka, Y., P. Parniewski, Z. Zwolska, M. Kai, T. Fujino, F. Kirikae, E. Toyota, K. Kudo, T. Kuratsuji, and T. Kirikae. 2004. Characterization of a trinucleotide repeat sequence (CGG)₃ and potential use in restriction fragment length polymorphism typing of *Mycobacterium tuberculosis*. *J. Clin. Microbiol.* 42:3538-3548.
13. Pfyffer, G. E., F. Palicova, and S. Rusch-Gerdes. 2002. Testing of susceptibility of *Mycobacterium tuberculosis* to pyrazinamide with the nonradiometric BACTEC MIGIT 960 system. *J. Clin. Microbiol.* 40:1670-1674.
14. Rossau, R., H. Traore, H. De Beenhouwer, W. Mijs, G. Jannes, P. De Rijk, and F. Portaels. 1997. Evaluation of the INNO-LiPA Rif. TB assay, a reverse hybridization assay for the simultaneous detection of *Mycobacterium tuberculosis* complex and its resistance to rifampin. *Antimicrob. Agents Chemother.* 41:2093-2098.
15. Salfinger, M., and G. E. Pfyffer. 1994. The new diagnostic mycobacteriology laboratory. *Eur. J. Clin. Microbiol. Infect. Dis.* 13:961-979.
16. Scorpio, A., P. Lindholm-Levy, L. Heifets, R. Gilman, S. Siddiqi, M. Cynamon, and Y. Zhang. 1997. Characterization of *pncA* mutations in pyrazinamide-resistant *Mycobacterium tuberculosis*. *Antimicrob. Agents Chemother.* 41:540-543.
17. Scorpio, A., and Y. Zhang. 1996. Mutations in *pncA*, a gene encoding pyrazinamidase/nicotinamidase, cause resistance to the antituberculous drug pyrazinamide in tubercle bacillus. *Nat. Med.* 2:662-667.
18. Sekiguchi, J., T. Miyoshi-Akiyama, E. Augustynowicz-Kopec, Z. Zwolska, F. Kirikae, E. Toyota, I. Kobayashi, K. Morita, K. Kudo, S. Kato, T. Kuratsuji, T. Mori, and T. Kirikae. 2007. Detection of multidrug resistance in *Mycobacterium tuberculosis*. *J. Clin. Microbiol.* 45:179-192.
19. Snider, D. E., Jr., J. Rogowski, M. Zierski, E. Bek, and M. W. Long. 1982. Successful intermittent treatment of smear-positive pulmonary tuberculosis in six months: a cooperative study in Poland. *Am. Rev. Respir. Dis.* 125:265-267.
20. Wayne, L. G. 1974. Simple pyrazinamidase and urease tests for routine identification of mycobacteria. *Am. Rev. Respir. Dis.* 109:147-151.
21. Zhang, Y., and D. Mitchison. 2003. The curious characteristics of pyrazinamide: a review. *Int. J. Tuberc. Lung Dis.* 7:6-21.
22. Zhang, Y., and A. Telenti. 2000. Genetics of drug resistance in *Mycobacterium tuberculosis*, p. 235-256. In G. F. Hatfull and W. R. Jacobs (ed.), *Molecular genetics of mycobacteria*. American Society for Microbiology, Washington, DC.